ISSN 0020-1685, Inorganic Materials, 2021, Vol. 57, No. 13, pp. 1319–1339. © Pleiades Publishing, Ltd., 2021.

Nanoscale Single-Crystal Silicon Carbide on Silicon and Unique Properties of This Material

S. A. Kukushkin[a], * and A. V. Osipov[a]

[a] *Institute for Problems of Mechanical Engineering, Russian Academy of Sciences, St. Petersburg, 199178 Russia*

**e-mail: sergey.a.kukushkin@gmail.com*

Received March 1, 2021; revised March 31, 2021; accepted April 5, 2021

Abstract—The paper reviews the latest advances in the growth of epitaxial SiC films on Si by the coordinated atomic substitution method. The conceptual issues and procedure of the new method for synthesizing epitaxial SiC films on Si are described. It is shown that this method significantly differs from the classical thin film growth schemes. Film growth in accordance with the classical mechanism is provided by deposition of atoms on the surface of a substrate. The new method consists in the coordinated atomic substitution of a portion of the atoms of the silicon matrix by carbon atoms to form an epitaxial silicon carbide film. The new growth method is compared with the classical thin film growth mechanisms. It is shown that the main distinctive feature of SiC films synthesized by this method is the formation of an excess concentration of silicon vacancies in it, whereas SiC grown by the standard methods comprises mostly carbon vacancies. It is shown that the interaction of carbon atoms and silicon vacancies leads to the formation of ordered ensembles of carbon–vacancy structures in SiC layers grown by the coordinated atomic substitution method. The formation of these structures is attributed to both the occurrence of a chemical substitution reaction and the contraction of the Si lattice cell during the transformation of it into a SiC lattice cell. The presence of carbon–vacancy structures in SiC imparts a number of new unique properties to the silicon carbide. In particular, a Si layer exhibiting the electronic properties of a "semimetal" is formed at the SiC–Si interface. In addition, carbon–vacancy structures provide unique optical, electrical, and magnetic properties. In particular, two quantum effects—a hysteresis of the static magnetic susceptibility and the occurrence of Aharonov–Bohm oscillations in the field dependences of the static magnetic susceptibility—are found to occur in weak magnetic fields at room temperature. The first of the effects is associated with the Meissner–Ochsenfeld effect; the second is associated with the presence of carbon–vacancy structures and microdefects in the form of nanotubes and micropores formed in these structures during SiC synthesis under the SiC layer.

Keywords: silicon carbide on silicon, silicon carbide, heterostructures, epitaxial films, heterogeneous reactions, substitution reactions, wide-gap semiconductors

DOI: 10.1134/S0020168521130021

CONTENTS

1. Introduction

2. Synthesis Procedure for Epitaxial SiC Films on Si by the Coordinated Atomic Substitution Method

3. The Main Physicochemical Processes That Occur during the Growth of Epitaxial SiC Films on Si by the Coordinated Atomic Substitution Method

4. The Main Instrumental Methods Used to Study the Crystal Structure, Morphology, and Properties of SiC Films on Si

5. The Main Distinctive Feature of SiC Synthesized by the Coordinated Atomic Substitution Method Is the Presence of Carbon–Vacancy Structures in It

6. Experimental Detection of Carbon–Vacancy Structures

7. Grounds for the Use of a Mixture of CO and SiH_4 Gases to Synthesize SiC by the Coordinated Atomic Substitution Method

8. Chemical Processes That Occur during the Topochemical Transformation of Si into SiC

9. Growth of an Epitaxial SiC Layer on the *n*- and *p*-Type Conductivity Si(100) Surface

10. Drift Mechanism of Epitaxy of SiC Films during their Growth by the Coordinated Atomic Substitution Method on a Crystalline Si Substrate: Diffusion Mechanism of CO and SiO Molecules in Si

11. The Polytypism of SiC

12. The Elastic Properties of SiC Films Synthesized on Si Substrates by the Coordinated Atomic Substitution Method

13. Anomalies of the Optical and Magnetic Properties of SiC Film Growth on Si by the Coordinated Atomic Substitution Method

14. Conclusions

References

1. INTRODUCTION

In 2008, a new method for synthesizing epitaxial films of silicon carbide (SiC) on silicon (Si) was theoretically predicted and experimentally validated in [1] and patented [2]. It should be noted that the development of this method was first reported on June 27, 2006, at the Russian Academy of Sciences at a meeting of the Bureau of the Department of Energy, Mechanical Engineering, Mechanics, and Control Processes of the Russian Academy of Sciences (resolution no. 62 of June 27, 2006) [3]. The method [1–3] is based on the chemical transformation (conversion) of the surface layers of silicon into epitaxial layers of silicon carbide through a chemical reaction between gaseous carbon monoxide (CO) and the surface of a silicon substrate in accordance with reaction (1):

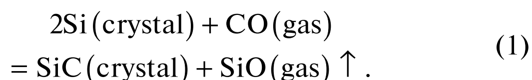

$$2\mathrm{Si}\,(\mathrm{crystal}) + \mathrm{CO}\,(\mathrm{gas}) = \mathrm{SiC}\,(\mathrm{crystal}) + \mathrm{SiO}\,(\mathrm{gas}) \uparrow . \quad (1)$$

In later reports, this method was referred to as the coordinated atomic substitution method [4]. The term “coordinated” means that new chemical bonds are formed simultaneously and consistently with the destruction of the old bonds. Later, a consistent theory was developed to describe the entire spectrum of interrelated physicochemical processes that occur during the topochemical transformation of Si into SiC [4–12].

Note that, as far back as 2005, the authors of [13–15] described and patented a method for synthesizing an epitaxial layer of SiC on Si by providing a direct contact between a silicon substrate and a polished carbon washer made of porous carbon with a diameter corresponding to the diameter of the silicon substrate. However, the conclusion made in [15] about the causes of the formation of SiC during this synthesis of SiC was not entirely correct. The authors of [15] believed that a SiC layer on Si is formed owing to the decomposition of the Si_2C gas on silicon. It was assumed that the Si_2C gas is formed through the interaction of Si atoms evaporating from the silicon substrate at high temperatures with the porous carbon of the carbon washer. Further studies [1–12] showed that, under conditions of this method, the SiC formation mechanism is almost completely identical to the mechanism developed in [1]. It was found that the porous carbon washer contained residual oxygen; at high temperatures, the residual oxygen was attached to carbon to form CO or, depending on the synthesis conditions, CO_2. After that, the $CO(CO_2)$ gas reacted with Si to form SiC. In terms of practical applications, this SiC film growth method was found to be insufficiently promising because of the presence of a significant amount of carbon, silicon vacancies, and etching pits emerging on the surface of the SiC layer. It is difficult to eliminate these defects in the case of growing SiC layers by this method. Therefore, subsequently, SiC layers were grown by the method described in [1–12]; it is based on the use of pure CO gas, rather than the CO_2 gas formed during the oxidation of porous carbon by atmospheric oxygen.

A detailed description of the SiC growth processes by the coordinated atomic substitution method that were conducted over the period from the start of the studies in 2004 to 2014 can be found in [10–12]. The cited reviews describe both theoretical and experimental studies and provide a detailed description of the setup for SiC growth. In addition, a number of purely technological procedures required for the formation of SiC layers with a high degree of crystal perfection are described in [10–12].

The above issues will not be the focus of this review. Here, we will only briefly describe the main technological outline of the SiC-to-Si transformation process and then describe new theoretical and experimental data on the growth and structure of SiC films that have been obtained since 2014.

2. SYNTHESIS PROCEDURE FOR EPITAXIAL SiC FILMS ON Si BY THE COORDINATED ATOMIC SUBSTITUTION METHOD

The synthesis of a SiC layer on Si is implemented on a special setup represented by a flow-type furnace with a quasi-closed reactor. A detailed design of this setup is described in [11, 12]. The design and major units of the setup are patented [16]. The setup provides the growth of SiC layers on Si substrates with a diameter of up to 40 mm. Silicon carbide films on substrates with a diameter of 51 (2"), 76 (3"), 102 (4"), 152 (6"), and 203 mm (8") are grown using a commercial furnace manufactured by Nabertherm; at our request, the furnace was partly modified by the company to provide the synthesis of SiC by the coordinated atomic substitution method. Figure 1 shows a photograph of a Nabertherm furnace with special additional inlets for CO, SiH_4, H_2, and Ar gases.

To grow a high-quality single-crystal SiC layer by the coordinated atomic substitution method, it is important to fulfill the following conditions: the silicon wafer surface on which the SiC film will be grown should not only be free of foreign impurities of organic matter, metals, and anions but also be smooth at the nanolevel and free even of an ultrathin (on the order of a few fractions of a nanometer) silicon dioxide (SiO_2) layer, which is typically formed during aqueous chemical etching and subsequent air storage. Otherwise, the occurrence of a chemical reaction between CO and Si containing SiO_2 on the surface will differ from the occurrence of the reaction described by Eq. (1). To provide the formation of an epitaxial SiC layer, before the occurrence of reaction (1), the Si surface should be prepared for the growth of SiC: it is necessary to obtain a surface that is smooth at the atomic level and remove even nanolayers of silicon dioxide from the surface of the silicon substrate. Our studies showed that the SiO_2

Fig. 1. Photo of a Nabertherm furnace with special additional inlets for CO, SiH_4, H_2, and Ar gases.

removal procedure should meet the following conditions:

(i) After the removal of the oxide, the Si surface should have a perfect crystal structure, while the densely packed Si(111) surface should be atomically smooth.

(ii) Etching pits should not appear at the site of dislocation outcrops. Etching pits can begin to vigorously develop and grow through the SiC film to form through channels extending from the silicon to the SiC film surface. The intergrowth of dislocations and their coalescence to form nanotubes lead to a violation of the structure of the SiC surface layer. The gaseous reaction product—SiO—erupts through these nanotubes to the SiC film surface to form structures that resemble volcanoes on the earth's surface [10]. It was found [17] that, even if the nanotubes do not emerge directly to the SiC film surface, yet are close to it, the elastic energy arising in this case has a significant effect on the surface structure of the SiC layers. If subsequently grown SiC layers containing these defects are used as buffer layers for growing films of aluminum (AlN) and gallium nitrides (GaN), then dislocation nanotubes will lead to the formation of so-called V-defects on the surface of the AlN and GaN films [17].

(iii) An important condition for the preparation of the Si surface for the growth of SiC is the absence of impurity particles of various origins, in particular, metal impurities, on the Si surface. This is particularly true for organic contaminants, because they can be involved in parasitic reactions during SiC synthesis.

(iv) An important aspect of the preparation of the Si surface for the growth of SiC is the development of a preparation procedure that would provide the possibility of long-term air storage of the wafers without their oxidation.

(v) Finally, the procedure should be fairly simple, accessible, and inexpensive to implement in research laboratories with the possibility of simultaneously

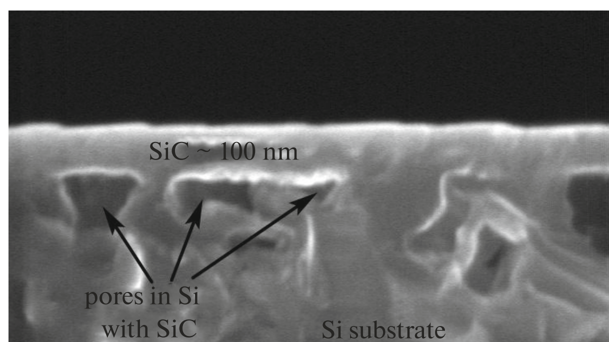

Fig. 2. Typical SEM micrograph of a face end cleavage of a SiC layer on the Si(111) surface; the SiC layer and pores in Si covered with SiC are clearly visible.

transferring it to an industrial scale. This technique was developed and described in [18] and patented [19]. In the cited reports, the well-known RCA procedure for cleaning the Si surface [20] was significantly modified. The method for cleaning and passivating the surface of silicon wafers of the (111), (110), and (100) orientations by hydride groups that was developed in [18, 19] makes it possible to provide a high purity and smoothness of the Si surface at the nanolevel during long-term storage of the wafers at room temperature in air. To provide a long-term protection of the Si surface from oxidation, a new composition of the passivating solution was developed. The solution formulation developed in [18, 19] is suitable for long-term storage and multiple passivation of silicon wafers. Before synthesizing the films, it is necessary to remove the protective layer of hydrogen from the Si surface. To this end, it is sufficient to anneal wafers with the (111) and (100) base surfaces in a vacuum at a temperature of 550°C for 1 min. To remove hydrogen from the vicinal (111) and (100) surfaces and from the (110) surface, the wafers should be annealed in a vacuum at a temperature of 580–600°C for 1 min.

Thus, the substrate should be cleaned of various contaminants, impurities, and SiO_2 before SiC synthesis. However, for laboratory experiments, it is quite sufficient to etch Si substrates in 5% HF for 5 min. In this case, before etching, the substrates should be subjected to grinding, polishing, and removal of organic impurities from their surface.

A SiC layer on Si is synthesized as follows. A silicon substrate in the form of a single-crystal silicon wafer with the surface covered with hydride groups, which is cut out taking into account the crystallographic orientation, is placed on a sample holder. After that, the reaction chamber is evacuated to a residual pressure of 10^{-2}–10^{-3} Pa to start the heating. At a temperature of about 550°C, silane (SiH_4) is introduced into the system; the wafer is held at this temperature for 1–2 min to remove the hydride groups (below, in discussing the special properties of SiC on Si, the reasons for the addition of SiH_4 to CO will be given). The SiH_4 flow rate is in a range of 0.25–0.35 sccm (below, the reasons for the addition of silane to CO to grow SiC from a mixture of these gases will be given). Next, the wafer is heated to a temperature of 850°C. At this temperature, the CO gas is introduced into the furnace at a pressure of 20–600 Pa. The CO flow rate is about 12 sccm. The synthesis temperature depends on the further use of the wafer with a SiC layer. If ultrathin SiC layers (1–10 nm) are required, then the synthesis temperature should not exceed 930–980°C. Standard layers will be formed at a temperature of about 1250–1290°C. To obtain thicker layers, the synthesis should be conducted at temperatures of 1330–1390°C. The synthesis time is 1–60 min depending on the necessity to obtain a particular structure of the SiC layer. Typically, at a short synthesis time, a large number of carbon–vacancy structures are formed [4, 10, 11, 21]; they will be discussed below. At a longer synthesis time, these structures are annealed and silicon carbide becomes more perfect. However, silicon carbide containing a high concentration of carbon–vacancy structures exhibits a number of unusual physicochemical properties and can be used to solve a number of applied problems, whereas annealed carbide can be used in another field of applied problems. Figure 2 shows a typical scanning electron microscope (SEM) image of a face cut of a SiC layer on Si. It clearly shows a continuous SiC layer and pores coated with SiC in Si.

Note that, for many research purposes, it is not at all necessary to use complex setups and it is not even necessary to directly use the CO gas to obtain SiC. If there is no need to obtain highly perfect SiC layers, it is quite sufficient to use polished graphite washers attached to silicon substrates, as in [13–15]. After that, these structures are placed in a furnace at a temperature of 1000–1390°C (depending on the necessity to obtain particular properties) and annealed in an air atmosphere or, better yet, in pure oxygen. The resulting CO gas will convert Si to SiC. CO_2 gas can also be used [2]. In this case, solid SiO_2 will be formed instead of SiO. Eventually, the SiC layer will contain a large amount of a polycrystalline phase; however, it is known that, with an increase in temperature, in the presence of carbon, CO_2 undergoes decomposition into CO. The resulting CO will undergo reaction (1). The higher the temperature, the larger the amount of CO and the higher the quality of the growing SiC layer.

The main chemical and physical processes that occur in the solid phase during the synthesis of SiC on Si by the coordinated atomic substitution method are described in detail in [10–12] and in the references in these reviews to particular reports. In addition, the cited reviews provide a detailed description of the thermodynamics and kinetics of the transformation of Si into SiC. Here, only a brief description of the main stages of this transformation will be given.

3. THE MAIN PHYSICOCHEMICAL PROCESSES THAT OCCUR DURING THE GROWTH OF EPITAXIAL SiC FILMS ON Si BY THE COORDINATED ATOMIC SUBSTITUTION METHOD

The coordinated atomic substitution method is based on the "assembly" of a new silicon carbide matrix based on the old silicon matrix via the partial substitution of carbon atoms for silicon atoms localized in the crystal matrix of the substrate. The SiC matrix is "assembled" via chemical reaction (1). Reaction (1) occurs in two stages [4–12, 21]. At the first stage, a silicon vacancy–carbon atom–silicon matrix ($C-V_{Si}$) intermediate state (counterpart of an activated complex) is formed in silicon. At this stage, carbon atoms are localized at the interstitial positions of the silicon matrix. The formation of a metastable superlattice near the silicon surface can be stated. At the second stage of the reaction, the superlattice is transformed into silicon carbide, while the disengaged vacancies merge into pores formed under the silicon carbide layer. In a crystal of cubic symmetry, these two dilatation centers (carbon atom and the silicon vacancy) undergo an elastic interaction with each other. If the dilatation dipoles are localized perpendicular to the (111) silicon plane, then they are attracted to each other [5–10]. In this case, almost the entire dilatational elastic energy arising from the introduction of a carbon atom and the formation of a vacancy undergoes relaxation [5–10, 21]. Since one of the stages of the transformation of Si into SiC is the formation of defects ($C-V_{Si}$), which undergo a mechanical elastic interaction, it was necessary to derive a formula for the energy of their interaction. Eventually, a theory of elastic interaction of two point defects in crystals of cubic and hexagonal symmetries was developed [5, 6, 22] and a formula for the interaction energy between two point defects in these crystals was derived. For cubic symmetry crystals, the interaction energy between two point defects $E_{int}(\cos\varphi(x,y,z))$ has the form [5, 6, 22]

$$E_{int}(\cos\varphi(x,y,z)) = -\frac{E_0\left(\cos^4\varphi_x + \cos^4\varphi_y + \cos^4\varphi_z - \frac{2}{5}\right)}{r^3}, \quad (2)$$

where $E_0 = 15K(3c_{11} - 4c_{44})\Omega^I\Omega^{II}\eta/8\pi(c_{12} + 2c_{44})$; $K = (c_{11} + 2c_{12})/3$ is the bulk modulus of elasticity (for Si, $K^{Si} = 0.98 \times 10^{11}$ N/m^2); c_{11}, c_{12}, and c_{44} are the elastic moduli of the cubic crystal; for Si, $c_{11} = 1.66 \times 10^{11}$ N/m^2, $c_{12} = 0.633 \times 10^{11}$ N/m^2, and $c_{44} = 0.796 \times 10^{11}$ N/m^2; $\eta = (c_{11} - c_{12} - 2c_{44})/c_{44}$ is the crystal anisotropy parameter; for Si, $\eta = -0.689$; Ω^I and Ω^{II} are associated with the difference between the volumes of the inclusion and the vacancy cavity; r is the distance between the defects; and $\cos\varphi_i = x_i/r$ are the direction cosines between the x, y, and z axes and the direction of the straight line connecting the centers of interacting defects. The $\cos^4\varphi_x + \cos^4\varphi_y + \cos^4\varphi_z - 3/5$ value has a maximum in the (100) direction of 0.4, a minimum in the $\langle 111\rangle$ direction of –0.27, and a saddle point of –0.1 in the (110) direction; therefore, the highest attraction between point defects takes place if these defects lie in interstices localized along the $\langle 110\rangle$ directions of silicon, i.e., if the carbon atom is localized at an interstitial position under the (111) planes along the $(\bar{1}10)$ plane, and the vacancy with respect to this atom should be localized along the $\langle 111\rangle$ direction. In this case, the attraction between the silicon vacancy and the carbon atom will be maximal. The interaction energy is inversely proportional to the cube of the distance between the defects. This system is a stable complex, which, by analogy with an electric dipole, is referred to as a dilatation dipole [5, 6]. Formula (2) in the correct form was first derived in [22]. Note that Eshelby was the first who studied the interaction between two point dipoles in cubic symmetry crystals [23]. Later, it was found that the sign of the interaction energy determined by Eshelby should be replaced by the opposite sign. In the derivation of a formula for the interaction energy from the anisotropic tensor Green's function developed by Lifshitz and Rosentsveig [24], the sign of the interaction between point defects was also incorrect. A detailed discussion of the problem of interaction between point defects in anisotropic media can be found in [4, 5, 22, 23, 25].

In the case of the formation of interacting defects in the bulk of a crystal, the total elastic energy of the crystal has the form [6]

$$W(\cos\varphi(x,y,z)) = E_C + E_V + E_{int}(\cos\varphi(x,y,z)), \quad (3)$$

where E_C and E_V are the energies of the elastic distortion of the lattice by a vacancy and a carbon atom, respectively, $E_{C,V} = \frac{2\mu^{Si}K^d}{3K^d + 4\mu^{Si}}\frac{(V^d - V^{Si,m})^2}{3V^{Si}}$; the volume per atom in a silicon crystal is V^d is the volume occupied by the defect in silicon; $V^{Si,m}$ is the volume of the interstitial position in silicon; μ^{Si} is the shear modulus of Si, $\mu^{Si} = 5.2 \times 10^{10}$ N/m^2; K^d is the bulk modulus of elasticity of the point defect; since a carbon atom and a vacancy are modeled by point incompressible dilatation centers, their bulk moduli of elasticity can be set equal to $K^d = \infty$; and V^{Si} is the volume per atom in silicon, $V^{Si} \approx 2.0 \times 10^{-29}$ m^3. Calculations of the elastic energy values by formulas (2) and (3) can be found in [5, 6]. The calculations showed that dilatational elastic energy can undergo complete relaxation due to dipoles alone. The lifetime of dilatation dipoles at temperatures of 1100–1250°C is approximately ~10^{-1}–1 s; therefore, elastic dipoles additionally play the role of ordering centers of epitaxy. The localization of point defects along the $\langle 100\rangle$ direction leads to the

following: the defects, conversely, repel, dipoles are not formed, and the resulting high elastic energy makes the localization of defects along the ⟨100⟩ direction unfavorable; this factor leads to the misorientation of the layers.

Thus, at the first stage of the reaction, the CO molecule interacts with the surface of the silicon substrate and undergoes decomposition into a carbon atom and an oxygen atom. The oxygen atom undergoes a chemical reaction with a Si atom to form the SiO gas. The SiO gas is removed from the system, and a vacancy is formed at the site of the silicon atom of the substrate that was transformed into the SiO gas. The active (energetically excited) carbon released from the CO molecule owing to the chemical reaction is displaced to an interstitial position in the silicon lattice [4, 10, 21]. This stage can be written as follows:

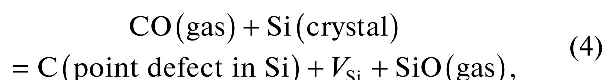

$$\begin{gathered}\mathrm{CO(gas)} + \mathrm{Si(crystal)} \\ = \mathrm{C(point\ defect\ in\ Si)} + V_{\mathrm{Si}} + \mathrm{SiO(gas)},\end{gathered} \tag{4}$$

where V_{Si} is the silicon vacancy. It is this stage where the intermediate phase of the so-called “precarbide” silicon is formed. This phase is represented by silicon saturated with vapors of C + V_{Si} defects. According to (4), pairs of point dilatation defects C and V_{Si} are always formed and disappear in pairs. Precarbide silicon is actually silicon in which every second Si atom is replaced by a C atom via reaction (4). Thus, one Si cell contains four pairs of dilatation defects C + V_{Si}; that is, in precarbide silicon, everything is already ready for the transformation of silicon into silicon carbide. This process occurs at the next stage of the reaction, which is described by Eq. (5):

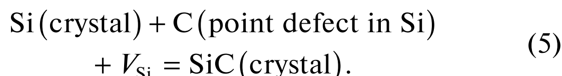

$$\begin{gathered}\mathrm{Si(crystal)} + \mathrm{C(point\ defect\ in\ Si)} \\ + V_{\mathrm{Si}} = \mathrm{SiC(crystal)}.\end{gathered} \tag{5}$$

At this stage, the carbon atoms undergo coordinated displacement toward the silicon vacancies to form silicon carbide. The final topochemical reaction (1) is a sum of stages (4) and (5). It is the elastic interaction between pairs of point dilatation defects C and V_{Si} that determines the kinetics of reaction (1). It is significant that the first-order phase transition (5) occurs in a coordinated manner; that is, the breaking of old bonds between the atoms and the formation of new bonds occur simultaneously and consistently; it is actually this factor that provides a high crystalline perfection of the silicon carbide film. This transformation is always accompanied by the formation of voids, because the volume of the Si cell is two times larger that the volume of the SiC cell. The length of all bonds decreases by 20%, namely, from 2.35 to 1.88 nm. The first-order phase transition (5) occurs layer by layer; that is, layers of precarbide silicon are simultaneously transformed into SiC, while the film is displaced perpendicular to the substrate surface. The constant of chemical reaction (5) is approximately two orders of magnitude higher than the constant of chemical reaction (4); therefore, stage (5) occurs significantly later and faster than stage (4). This factor can be responsible for the fact that the resulting SiC film is fairly uniform in thickness and does not have visible voids. All voids are localized in silicon under the SiC film [4–12, 21].

A remarkable feature of reaction (1) is that this reaction ends with the formation of silicon carbide and does not occur further to the formation of carbon or even diamond. This fact is attributed to both stage (4) and stage (5). The occurrence of reaction (4) requires the presence of a “free space” in the silicon cell for the localization of a carbon atom in it. Only one carbon atom can fit inside this cell. It is this factor that is responsible for the fact that only four atoms in the silicon lattice, rather than all eight atoms, can be substituted. Otherwise, the resulting lattice will be a diamond lattice with an extremely high elastic stretch ratio. To this end, it would be necessary to overcome an extremely high activation energy. This reaction cannot occur under these conditions. Even a simpler reaction of localization of a carbon atom in each crystal cell of silicon cannot occur. Carbon atoms can be localized inside the cell only if one silicon atom is removed from the silicon cell, i.e., if the cell contains a silicon vacancy. In addition, point defects (carbon and vacancy) should be strictly localized along a certain crystallographic direction in Si, namely, [111]. Only in this case, owing to the elastic mechanical attraction of dilatation defects, is their total elastic energy zero. Otherwise and along other crystallographic directions in Si, reaction (4) does not occur. Thus, reaction (4) not only “selects” four Si atoms that are necessary for it but also “isolates” a single direction in the crystal space along which the future SiC crystal lattice is formed. However, reaction (4) is insufficient for the transition of Si to SiC. The SiC synthesis process ends with reaction (5). For the occurrence of reaction (5), it is significant that the five crystal cells of SiC that are formed owing to this reaction almost exactly coincide with four cells of Si [4, 10]. As a consequence, the atomic displacement reaction (5) occurs with minimum energy consumption. It is reaction (5) that completes the “final matching” of the crystal lattices. If, for one reason or another, all eight Si atoms, rather than four of them, were replaced via reaction (4), then reaction (5) would not occur because of the high elastic energy of lattice mismatch (as in the case of diamond). For this reason, graphite cannot be formed either, because it has a hexagonal lattice and other cell parameters.

4. THE MAIN INSTRUMENTAL METHODS USED TO STUDY THE CRYSTAL STRUCTURE, MORPHOLOGY, AND PROPERTIES OF SiC FILMS ON Si

The reports summarized in [10–12] provide a detailed description of many experimental studies of SiC/Si samples. To validate this growth method, we

grew and studied several thousand samples of SC films on Si. The films were studied by the following methods: spectral ellipsometry on a J.A. Woollam M2000-RCE ellipsometer in a range of 0.7–6.5 eV, Raman spectroscopy on a Witec Alpha 300R confocal Raman microscope, reflection high-energy electron diffraction (RHEED) at an electron energy of 50 keV, and X-ray diffraction (XRD) analysis (both diffraction patterns in the ω–2θ mode and the rocking curves in the ω–θ mode were recorded). The surface of films was studied by atomic force microscopy and using a Zygo New View 6000 profilometer. The surface of the SiC/Si layers and the surface of face end cleavages were studied by SEM on a microscope equipped with an energy dispersive X-ray spectrometer, which made it possible to determine the chemical composition of the layers. The interface and defects in the layers were studied by high-resolution tunneling electron microscopy. Many samples were studied by Rutherford backscattering spectrometry using ion beams of helium and hydrogen [26] and by infrared (IR) spectroscopy using both a Bruker IFS-113v Fourier transform IR spectrometer and a Nicolet iS-50 IR spectrometer (Thermo Scientific, United States) [27–29]. In addition, the SiC/Si samples were studied by the X-ray reflectometry method [28, 29]. The photoemission studies of the samples were conducted on a BESSY II synchrotron at Helmholtz Zentrum in Berlin (Germany) using synchrotron radiation with photon energies in a range of 80–450 eV [30–32].

5. THE MAIN DISTINCTIVE FEATURE OF SiC SYNTHESIZED BY THE COORDINATED ATOMIC SUBSTITUTION METHOD IS THE PRESENCE OF CARBON–VACANCY STRUCTURES IN IT

The main conclusion that can be drawn from the conducted studies and measurements is as follows. The main distinctive feature of SiC synthesized from Si by the coordinated atomic substitution method is that, depending on the synthesis conditions, it contains silicon vacancies in an amount of 0.5–5%. It is the presence of silicon vacancies that is a distinctive feature that determines all the main properties of converted SiC from SiC grown by standard methods. Common SiC contains only carbon vacancies [33]. This feature is attributed to the fact that the energy for the formation of a silicon vacancy in SiC is on the order of ~8.7 eV, whereas the respective parameter for a carbon vacancy is ~4.6 eV. In SiC synthesized by the coordinated atomic substitution method, conversely, excess silicon vacancies are formed, and several processes are responsible for this formation.

The first factor, which is probably the most important, is the formation of vacancies in the silicon substrate subjected to heating in a vacuum to the SiC growth stage. The number of vacancies and the thickness of the layer where they were formed significantly depend on the temperature of the Si substrate and the heating time (energy for the formation of a vacancy in silicon is ~3.5 eV). One minute of heating at T = 1350°C is sufficient for the formation of a surface layer with vacancies with a thickness of about 1 μm or more. Subsequently, these vacancies can be transformed into silicon vacancies in SiC directly during the coordinated atomic substitution; they can also diffuse from Si to SiC after the SiC growth process. The second factor leading to an excess amount of Si vacancies is stages (4) and (5) of chemical reaction (1). During reaction (5), Si undergoes contraction and subsequent transformation into SiC. The 3C-SiC unit cell volume is almost two times smaller than the Si unit cell volume. At the moment of contraction, the initial coherence is violated and occurs only at places where every fifth SiC cell coincides with the fourth Si cell. Note that the distance between the C atoms along the (111) plane projected onto the $(11\bar{2})$ plane in SiC is 3.08 Å [10]. The respective distance between Si atoms in silicon is 3.84 Å. Hence, the distance between the planes of five cells in SiC is 15.40 Å, and the distance between four cells in Si is 15.36 Å. It was proven [10, 12] that it is the conjugation of every fifth and fourth crystal cell of Si and SiC that leads to the epitaxial orientation of the SiC film. According to [10, 11], the other bonds at the interface between SiC and Si are broken; pores are formed at these sites under the SiC layer (see figures in [10, 11]). Thus, coherent conjugation between the film and the substrate occurs only at places where every fifth SiC cell does not completely coincide with the fourth Si cell. The deformation arising from the difference between these parameters is negligible: it is 0.3%. It was shown [34] that, if the lattice parameters of the film and the substrate do not exceed 1%, then complete coherence between the film and the substrate can be preserved and defects will not be formed in the film, as observed experimentally for Si–SiC [35]. Despite the small deformation value, it leads to the occurrence of fairly high elastic stresses. An elementary calculation taking into account the above elastic constants shows, for example, that the radial component of elastic stresses is $\sigma_{rr} = -0.8$ GPa [36]. Hence, it is no longer the SiC film that has a large lattice parameter with respect to that of the original silicon substrate; on the contrary, the new ordering substrate (four silicon cells with pores under their surface) has a large lattice parameter. Thus, the substrate will compress the SiC film, rather than stretch it. It was shown [36] that, at a Si substrate thickness of about 300 μm and a SiC film thickness of 100 nm, stresses of 0.8 GPa lead to a wafer bending radius of $R = -270$ m. Thus, the SiC film will be stretched, and tensile elastic stresses tending to return the film to the original state will appear in it. This finding is in complete agreement with the experimental results [35, 37].

The third factor of the appearance of silicon vacancies in SiC is associated with the Gorsky's mechano-

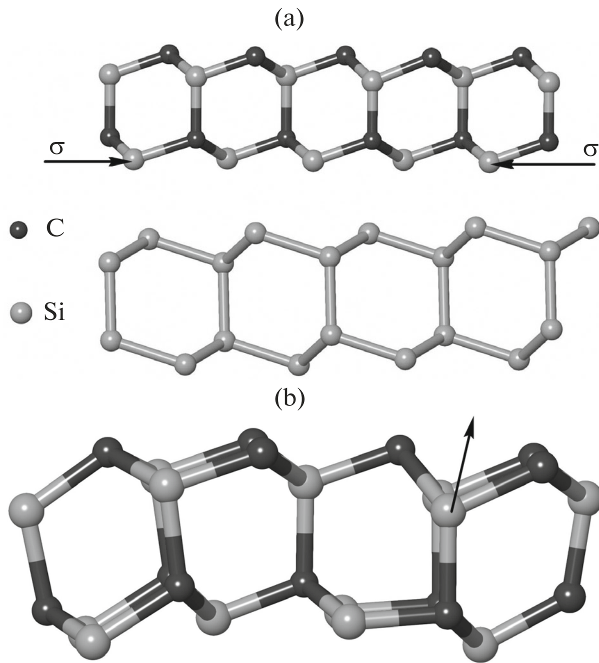

Fig. 3. Schematic representation of the Gorsky effect that occurs during the growth of SiC on Si by the coordinated atomic substitution method: (a) the initial structure of the Si substrate projected onto the $(11\overline{2})$ plane with four Si crystal cells (bottom figure) and five crystal cells of the SiC film projected onto the $(11\overline{2})$ plane (top figure) before the action of elastic deformations (arrows conventionally indicate the direction of application of mechanical stresses σ; small dark spheres denote C atoms; large gray spheres denote Si atoms) and (b) four SiC crystal cells stretched at the top and compressed at the bottom (arrow schematically indicates the evaporating Si atom).

chemical effect [38]. Since Si atoms in SiC are larger than C atoms, it is these atoms that will be pushed out by elastic stresses to the surface of the SiC layer to form vacancies in the silicon sublattice. The occurrence of the mechanochemical effect (Gorsky effect) is associated with the mechanism of ascending diffusion caused by the appearance of a gradient of elastic compressive stresses arising during film synthesis by the coordinated atomic substitution method. As a consequence, the atoms undergo a redistribution over the film thickness. The Si atoms emerging from the SiC film onto the film surface will evaporate and interact with CO to form another—disordered—SiC layer. In this case, excess silicon vacancies are formed in the surface layer of SiC. Figure 3 shows a schematic representation of the Gorsky effect that occurs during the growth of SiC films on Si. According to our reckoning, it is the Gorsky effect that leads to an asymmetry in the evaporation of Si and C atoms from the SiC film, because the sizes of these atoms significantly differ. An asymmetry in the evaporation of atoms leads to an asymmetry of the composition over the thickness of the SiC film. The activation energy for the emergence of Si and C atoms to the film surface and the formation of V_{Si} and V_C vacancies according to Schottky will be different for a stressed and unstressed film; this factor will lead to an asymmetry in their densities. This means that silicon will leave the Si sublattice, and the sublattice will be enriched in silicon vacancies, which will diffuse deep into the SiC layer.

The Gorsky effect can also arise during the cooling of a Si wafer with a SiC layer owing to a difference in the thermal expansion coefficients of the film and the substrate. In fact, the thermal expansion coefficient of the 3C-SiC polytype at $T = 1250°C$ is $\alpha^{3C\text{-}SiC} \approx 3.9 \times 10^{-6}\ K^{-1}$ [39]. Hence, the longitudinal thermal stresses

$$\sigma_T = \frac{\Upsilon^{SiC}}{1 - V^{SiC}}(\alpha^{Si} - \alpha^{SiC})\Delta T, \tag{6}$$

where Young's modulus of SiC is $\Upsilon^{3C\text{-}SiC} \sim 440$ GPa [39] and the Poisson ratio is $\nu^{3C\text{-}SiC} = 0.17$ [39]. Hence, during cooling from the synthesis temperature of $T = 1300°C$ to room temperature, elastic thermal stresses on the order of $\sigma_T^{3C-SiC} \sim -0.9$ GPa will appear in the film. Note that the Gorsky effect [38] is also referred to as ascending diffusion [36], because, in many cases, it leads to diffusion toward increasing the concentration, rather than toward decreasing it. In a general case, the ascending diffusion flux of Si atoms from silicon carbide I_{Si} under the action of stresses in the Si sublattice will be

$$I_{Si} = -N_{Si}\frac{D_{Si}\partial\sigma}{k_B T\partial x}\omega^{Si}, \tag{7}$$

where D_{Si} is the diffusion coefficient of Si over the silicon sublattice; N_{Si} is the density of silicon atoms in the silicon carbide sublattice, $N_{Si} \approx 4.83 \times 10^{28}\ m^{-3}$; σ is the mechanical stresses arising from both the difference in the crystal cell parameters of silicon and silicon carbide and the difference in the thermal expansion coefficients of Si and SiC; and ω^{Si} is the volume of the Si atom, $\omega^{Si} \approx 7 \times 10^{-30}\ m^3$. According to the conclusions of [36], in epitaxial films, at a temperature of 1300°C, the diffusion coefficient of Si in SiC single crystals is on the order of $D_{Si} \sim 10^{-17}\ m^2\ s^{-1}$. Hence, the flux of silicon atoms I_{Si} arising under the action of elastic stresses at the synthesis temperature in a SiC film with a thickness of about $H \sim 100$ nm is estimated at $I_{Si} \sim 10^{18}\ m^{-2}\ s^{-1}$.

It is significant that the formation of silicon vacancies in SiC occurs at fairly high temperatures of $T = 1100–1400°C$. Calculations conducted by the methods of quantum chemistry [43] show that it is favorable for a carbon atom adjacent to the vacancy to be displaced almost to the site of a silicon vacancy to form a nearly planar cluster of four carbon atoms (Fig. 4). Above and below the initial position of the carbon atom displaced to the silicon vacancy, two voids—each

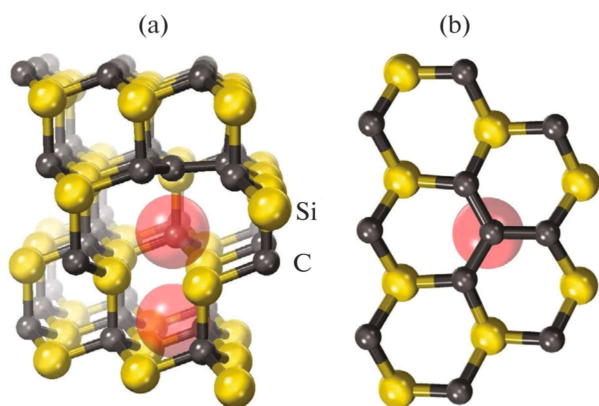

Fig. 4. Carbon–vacancy structure in SiC grown by the coordinated atomic substitution method: (a) a nearly planar cluster of four C atoms formed owing to the displacement of the C atom in the ⟨111⟩ direction (from bottom to top) to the site of the silicon vacancy and two voids (shown in red) above and below the initial position of the C atom (vertical axis corresponds to the ⟨111⟩ direction) and (b) the top view of the same structure.

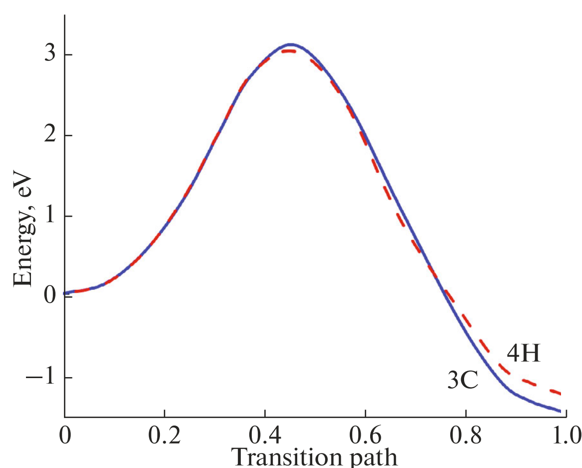

Fig. 5. Energy profile of the transformation of a silicon vacancy into a carbon–vacancy structure calculated in [21] for two SiC polytypes: (solid line) 3C and (dashed line) 4H. For the 4H polytype, an average profile is constructed for two asymmetric (i.e., more favorable) carbon–vacancy structures.

with a diameter of 2.15 Å—are formed; therefore, the resulting structure of a carbon cluster and two voids (this structure is always elongated in the ⟨111⟩ direction) is referred to as a carbon–vacancy structure (Fig. 4). The distance from the center of the carbon cluster to the first pore is 1.82 Å, while the distance between the two pores is 2.9 Å. The energy profile of the formation of this structure, i.e., the displacement of the carbon atom from the initial position to the most favorable position, is shown in Fig. 5 for two polytypes—3C and 4H. The gain from the formation of this carbon–vacancy structure is almost 1.5 eV, while the barrier that should be overcome is ~3 eV [43]. This means that, at the SiC growth temperature of $T = 1100°C$, the characteristic time to overcome the barrier is about 1 s; that is, during the growth of SiC by the coordinated atomic substitution method, almost all silicon vacancies are transformed into carbon–vacancy structures; this process fundamentally changes all properties of SiC [43]. It is this transformation that is responsible for the fact that ellipsometric studies always reveal excess carbon in SiC films synthesized by the atomic substitution method [8]; this carbon had no possibility to be formed chemically, because SiC was synthesized in that region of the phase diagram where the formation of carbon is excluded [40].

Studies of mechanochemical processes that occur during the growth of SiC on Si are of considerable importance for interpreting a number of events of diffusion and redistribution of atoms that occur in multilayer films and composite structures subjected to external or internal mechanical loads. This result substantively generalizes the Gorsky effect found earlier in solid solutions [38] to the case of chemical compounds. The results are important for a wide range of problems in physics, chemistry, and materials science and for designing and synthesizing new materials that can be used under the action of external elastic stresses and temperature differences.

It was found [41] that the rate of the chemical reaction of an ensemble of point defects in silicon (2) to form SiC significantly depends on the type and degree of doping of the original silicon. In particular, in silicon(111) of *p*-type conductivity, the formation of a structure in which carbon involved in reaction (5) is slightly displaced relative to the center of a silicon vacancy, instead of being completely combined with this vacancy, is favorable. The carbon atom that is slightly displaced into the interstitial space, instead of taking its place, exhibits the property of a donor impurity. As a consequence, it will have a positive charge. The silicon vacancy will exhibit the properties of an acceptor; that is, it will acquire a negative charge. As a consequence, an electric dipole will be formed and an electric field will arise in the SiC layer [42]. This situation is unstable, because a mechanochemical effect will occur and make some of the silicon atoms be displaced toward the film surface. This process will give rise to the generation of an internal electric field directed against the electric field of the dipole, which will lead to the formation of additional silicon vacancies. It was shown [21, 44] that the presence of silicon vacancies in SiC is indirectly confirmed by analysis of ellipsometric spectra, which unambiguously indicate the presence of approximately the same excess amounts of pyrolytic graphite and voids [44]. Ellipsometric analysis of silicon carbide grown by other methods has never revealed the presence of excess graphite.

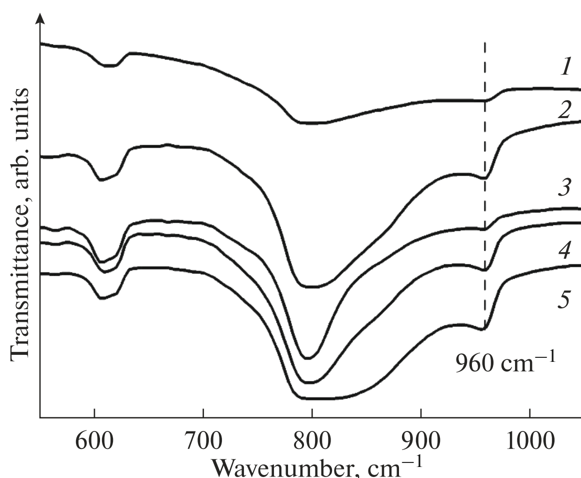

Fig. 6. Infrared transmission spectra of epitaxial SiC samples. The numbers of the curves correspond to the numbers of the samples grown on Si substrates of various orientations. Samples on Si(111) substrates without deviation from the (111) base plane and Si(100) substrates with a deviation from the (100) plane by 4° and at different synthesis temperatures were studied. However, for all the samples, the IR spectra exhibited a band in the region of 960 cm^{-1}, which was not observed earlier either for SiC single crystals or for SiC films grown on substrates made of silicon or other materials.

6. EXPERIMENTAL DETECTION OF CARBON–VACANCY STRUCTURES

In IR spectra, both in the absorption and transmission spectra of SiC/Si samples synthesized by the coordinated atomic substitution method, the authors of [27–29, 45] detected a band in the region of 960 cm^{-1}. The calculation made in [21] showed that this band corresponds to the vibration energy of a carbon cluster in a carbon–vacancy structure. It was found that the band at 960 cm^{-1} in the IR spectra of SiC films on Si, which corresponds to carbon–vacancy structures, is always present in SiC films grown in an atmosphere of pure carbon monoxide (CO) or in a mixture of CO and silane (SiH_4) on Si substrates characterized by different orientations and levels and types of doping. Figure 6 shows, as a case in point, the IR transmission spectra of samples of epitaxial SiC layers grown on Si(111) substrates without deviation from the (111) base plane and Si(100) substrates with a deviation from the (100) plane by 4° and at different synthesis temperatures. For all the samples, the studies revealed the presence of a band lying in the region of 960 cm^{-1} in the IR spectra; this band was not previously observed either in SiC single crystals or in SiC films grown on substrates made of silicon or other materials. It was found that the IR spectra of SiC films synthesized at an optimum ratio of the pressures of CO and trichlorosilane ($SiHCl_3$) gases do not exhibit an absorption band in the region of 960 cm^{-1}. Experiments conducted by IR spectroscopy and spectral ellipsometry revealed a fundamental difference in the mechanisms of formation of SiC films in a CO atmosphere with the addition of SiH_4 and in a CO atmosphere with the addition of $SiHCl_3$. Thus, the theoretical conclusion about the formation of carbon–vacancy structures in silicon carbide films grown by the atomic substitution method has been experimentally confirmed.

Photoemission studies of SiC/Si films were conducted on the BESSY II synchrotron at Helmholtz Zentrum in Berlin (Germany) using synchrotron radiation with photon energies in a range of 80–450 eV in a series of studies [30–32]. Thus, the authors of [32] studied the electronic properties of the nanointerface of Ba/SiC/Si(111) vicinal surfaces with a deviation by 8° from the (111) Si plane by the photoelectron spectroscopy method using synchrotron radiation. Experiments were conducted in situ in an ultrahigh vacuum for submonolayer coatings of Ba on SiC/Si(111)-8° samples. It was found that the adsorption of Ba causes significant changes in the spectrum of the C 1*s* core level. It was shown that the effect is attributed to the formation of a new, previously unknown, carbon nanostructure. It was found that the nanostructure is formed exclusively on the vicinal surfaces of SiC in the presence of stabilizing adsorbed Ba metal atoms and consists of carbon rings, in which chemical bonds are similar in nature to bonds inherent in aromatic compounds. It was found that a key role in the formation of this structure is played by carbon–vacancy structures.

7. GROUNDS FOR THE USE OF A MIXTURE OF CO AND SiH_4 GASES TO SYNTHESIZE SiC BY THE COORDINATED ATOMIC SUBSTITUTION METHOD

It was found above that, during the transformation of Si in to SiC, the following processes leading to the loss of silicon occur.

The first process in which the loss of Si occurs is stage (4) of chemical reaction (1). This stage is closely related to stage (5), at which the transformation of Si into SiC actually occurs with a simultaneous almost twofold contraction. The contraction gives rise to giant compressive stresses on the order of 100–200 GPa. Compression occurs for a short time—10^{-4} s. At the moment of compression, a powerful ejection of silicon takes place. In this case, contraction cavities, pores, and, certainly, vacancies are typically formed. A detailed theory of this contraction accompanied by loss of silicon is described in [10]. It is also shown there that the transformation consists of two closely related processes. One of the processes, which is referred to in [10] as the guiding transformation, is chemical reaction (4), which prepares transformation (5). The second process is referred to in [10] as the guided phase transformation. During the guided transforma-

tion, reaction (5) occurs; it leads to the exfoliation of the new SiC phase from the silicon matrix. At this stage, a single nucleus consisting of SiC and the surrounding exfoliation cavities (contraction pores) and pores in Si typically coated with SiC are formed. In this case, excess carbon having various forms and structures can be present in the SiC layer or directly on the layer surface. Exfoliation cavities are formed either owing to the generation of vacancies at the interface between Si saturated with elastic dipoles and Si (interface in the planar plane) under the action of tensile stresses and their transformation into a pore [46] or owing to the formation of dislocation loops [47]. On the stepped Si surfaces, which are also referred to as vicinal surfaces, instead of the formation of contraction cavities, their "folding" (similar to accordion bellows) with the simultaneous "ejection" of a portion of silicon will occur. The theory of this transformation was also constructed in [10]. The second process in which the loss of Si occurs is the above-discussed mechanochemical effect.

If the loss of silicon is not compensated for immediately during SiC synthesis, then the layer will be characterized by roughness, the presence of contraction pores, and a high density of carbon–vacancy structures. To eliminate this problem, an additional amount of silicon should be supplied to the system together with CO. To this end, different methods can be used. For example, an additional amount of Si can be supplied in the vapor phase (in this case, additional defects can be formed). Near the substrate, Si in a powdery state can be localized; it will evaporate. Various silicon-containing gases, such as SiH_4 or trichloromonosilane $SiHCl_3$, can be supplied. In addition, to provide the formation of a smoother surface, we always place two identical Si wafers opposite each other at a distance of about 1–5 mm (this is indirectly associated with the mean free path of an atom in the Si gas phase at the pressure at which growth occurs). Note that the addition of the $SiHCl_3$ gas leads to a more significant suppression of the formation of carbon–vacancy structures compared with the case of SiH_4.

In addition, $SiHCl_3$ plays another important role. The fact is that, if in reaction (1) the total critical pressure of gases (which, in particular, under equilibrium conditions at $T = 1300°C$, is $p_{cr} = 1.3$ Torr) is exceeded [1, 10], then, instead of reaction (1), another reaction can occur [36]:

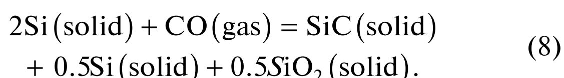

$$\begin{aligned}2\mathrm{Si}(\mathrm{solid}) + \mathrm{CO}(\mathrm{gas}) &= \mathrm{SiC}(\mathrm{solid})\\ &+ 0.5\mathrm{Si}(\mathrm{solid}) + 0.5\mathrm{SiO_2}(\mathrm{solid}).\end{aligned} \tag{8}$$

The fact is that, according to [36], upon the addition of the $SiHCl_3$ gas to CO (for example, in an amount of 1/8 of the amount of CO in a molar ratio), instead of reaction (1), at a pressure of $p = 1.6$ Torr and a temperature of $T = 1300°C$, the equilibrium reaction of SiC formation will occur as follows:

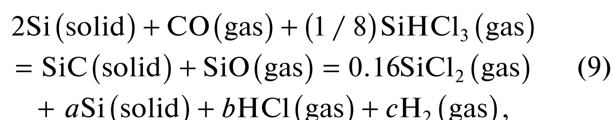

$$\begin{aligned}&2\mathrm{Si}(\mathrm{solid}) + \mathrm{CO}(\mathrm{gas}) + (1/8)\mathrm{SiHCl_3}(\mathrm{gas})\\ &= \mathrm{SiC}(\mathrm{solid}) + \mathrm{SiO}(\mathrm{gas}) = 0.16\mathrm{SiCl_2}(\mathrm{gas})\\ &+ a\mathrm{Si}(\mathrm{solid}) + b\mathrm{HCl}(\mathrm{gas}) + c\mathrm{H_2}(\mathrm{gas}),\end{aligned} \tag{9}$$

where a, b, and c are constants from 0.02 to 0.05. Unfortunately, additional chloride-containing substances released during this reaction interact with the gas distribution system and thereby lead to a rapid failure of the system, at least under our laboratory conditions. Therefore, we use only silane and the second—adjacent—silicon wafer as additional sources of silicon.

8. CHEMICAL PROCESSES THAT OCCUR DURING THE TOPOCHEMICAL TRANSFORMATION OF Si INTO SiC

The equilibrium state in a system of three elements—silicon Si, carbon C, and oxygen O—was calculated in terms of the thermodynamics of chemical reactions in [40, 48]. It was shown that, in the actual temperature range of $1000°C < T < 1400°C$, the system, which consists of crystalline Si and the CO gas at the initial moment of time, tends to an equilibrium state from a mixture of four solid phases—Si, C, SiC, and SiO_2—and an equilibrium vapor above them, which mostly consists of SiO, CO, Si, and CO_2. Equilibrium partial pressures of all the gases were calculated. It was shown that this equilibrium has one degree of freedom; therefore, the equilibrium partial pressures of all the gases depend only on temperature. An optimum mode for the growth of SiC films from a Si substrate by the atomic substitution method was proposed; in this mode, only a single SiC phase grows, while C and SiO_2 phases are not formed. In this mode, the partial pressure of CO should be equal to the equilibrium pressure, and the partial pressure of SiO should be slightly lower than the equilibrium pressure. It was shown that the best conditions for growing pure SiC are conditions that are far from thermodynamic equilibrium. Using the methods of linear algebra and the example of a heterogeneous transformation of Si to SiC during a chemical reaction with carbon monoxide, the basis of independent (base) chemical reactions was found and the pressure–flow phase diagram describing the composition and structure of the new solid phase was calculated [40]. The diagram is shown in Fig. 7. The effect of the anisotropy of elastic fields arising during the chemical transformation of one solid phase into another on the constants of chemical reactions has been taken into account for the first time. The diagram shown in Fig. 7 suggests the following. The best conditions for growing pure SiC are conditions that are far from the thermodynamic equilibrium of phases. The CO pressure should be 2–3 times lower than the equilibrium pressure in the reaction in order to avoid the appearance of carbon, while the gas flow rate in the system should be sufficiently high to exclude the possible formation of SiO_2. It should be

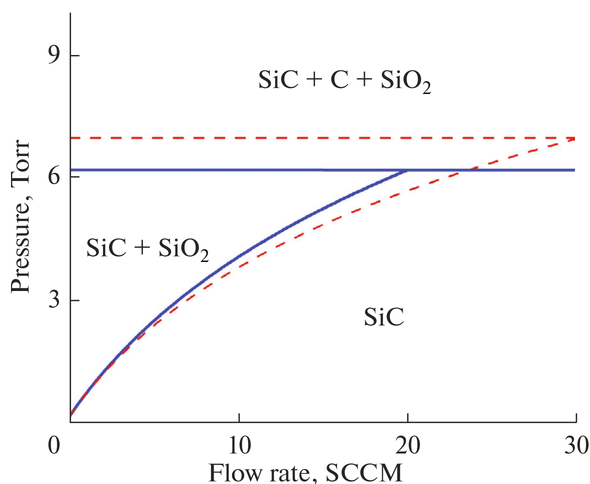

Fig. 7. Pressure–flow rate phase diagram describing the solid phase composition after a topochemical transformation in a vacuum furnace [11, 12, 16]. The solid and dashed lines correspond to $T = 1200$ and 1210°C, respectively.

noted that the constant of reaction (1) is affected by at least two additional effects. One of the effects is associated with the interaction of vacancies with the Si–SiC interface [25]. The other effect is associated with the fact that vacancies are an amphoteric impurity in a semiconductor and therefore can acquire different charges depending on the surface direction and the silicon conductivity type.

9. GROWTH OF AN EPITAXIAL SiC LAYER ON THE *n*- AND *p*-TYPE CONDUCTIVITY Si(100) SURFACE

As noted above, a distinctive feature of the coordinated atomic substitution method is that, regardless of the initial crystallographic plane of Si on which SiC was synthesized, the [111] plane is necessarily formed as one of the planes. This effect is attributed to the fact that the above-discussed carbon–vacancy structures are always localized along the ⟨111⟩ direction and lie in the [−110] plane perpendicular to the (111) plane. Further, after the formation of elastic dipoles, the formation of SiC occurs in accordance with reaction (5). In this case, contraction with the separation of the SiC nucleus from the Si matrix with the simultaneous formation of contraction cavities (pores) is observed. A theory of the formation of contraction cavities was constructed in [10, 41]; the theory is based on the model of pore nucleation from an ensemble of vacancies arising under the action of a tensile load [46]. The exfoliation of one material from another can also be caused by the formation of partial dislocations in the slip planes and the nucleation of vacancy dislocation loops [47]. It is known [49] that, at temperatures exceeding 0.5 of the melting point of the crystal (in our case, during SiC synthesis, this condition is necessarily satisfied for Si), the slip planes in crystals with a diamond lattice is the family of (111) planes, and the slipping motion occurs along the ⟨110⟩ directions. Therefore, on a smooth silicon (100) surface, SiC of the (100) orientation cannot be nucleated. However, nature acts elsewise. During conversion, the (100) face of Si is transformed into a SiC face consisting of a large number of facets resembling sawtooth structures, the side faces of which are covered with the (111), (110), and (210) planes, as shown in Fig. 8 [41]. The angle between the direction of the (100) face and the (111) faces is 54°44′. Any arbitrarily small deviation of the (100) face from this direction makes it vicinal and thereby leads to the instantaneous formation of an extremely thin (several atomic layers) film.

A different picture will be observed, if SiC is grown by the coordinated atomic substitution method on the (100) surface misoriented by 2°–7° in the ⟨011⟩ direction. If this surface is heated to a temperature above 600°C, then the (100) plane of silicon will be covered with steps. The terraces of this structure will be the (100) planes, and the steps will be limited to the (011) planes. The presence of "channels" along the ⟨011⟩ directions in the silicon lattice is observed; this fact is attributed to the specific features of the crystallographic structure of the Si lattice. Therefore, the CO molecules penetrate deep into Si along this direction perpendicular to the steps. The Si surface is saturated with CO and, as described above, Si and CO react to form an intermediate state, which is transformed into SiC. During this transformation, a portion of the Si evaporates from the (011) step and the (111) step of SiC is formed [41]. This process is schematically shown in Fig. 9. This transformation removes the "degeneracy" inherent in the nondeviated (100) face and leads to the formation of facets consisting of the (111) faces of SiC; these facets are localized on the former (011) steps instead of being randomly localized, as on the (100) face. It is only natural that these faces also make an angle of ~55° with the (100) face and an angle of ~35° with the (011) face. Since the attraction between a silicon vacancy and a carbon atom in the silicon matrix is maximal along the ⟨111⟩ direction, a portion of the (011) Si step can be transformed into a (112) SiC offset. It is known that the angle between the (112) and (100) planes in a cubic crystal with a diamond lattice is ~35°. The result is the formation of a longitudinal wedge-shaped offset of silicon carbide, which has a top protruding above the step platform and an inclined face extending to the platform of the low-lying step to form a slope. These SiC facets resemble "fish scales" or "knightly chain mail," the plates of which are close-fitted to each other [41]. Figure 10 shows an experimentally obtained atomic force microscopy image of a SiC layer covered with (111) facets grown on a vicinal Si(100) surface deviated from the ⟨100⟩ direction toward ⟨011⟩ by 4°. As a consequence, the Si(100) surface is covered with an array of parallel wedge-shaped steps having the form of triangular prisms (side faces of

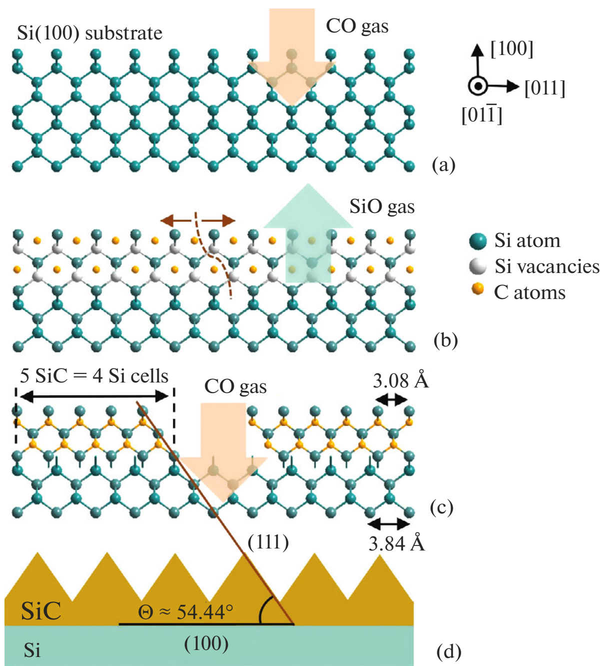

Fig. 8. Schematic representation of the successive stages of transformation of the singular Si(100) surface into SiC covered with facets during the exposure of the Si surface to the CO gas in accordance with reaction (1): (a) bringing the Si(100) surface in contact with the CO gas; (b) the first stage of the reaction, namely, the removal of Si using the SiO gas and the formation of dilatation dipoles (C–V_{Si}); (c) the phase transition from the intermediate state of silicon into a SiC layer; and (d) the formation of a sawtooth surface of the SiC film covered with (111) facets; θ = 54°44′ is the angle between the SiC(111) facet and the Si(100) surface.

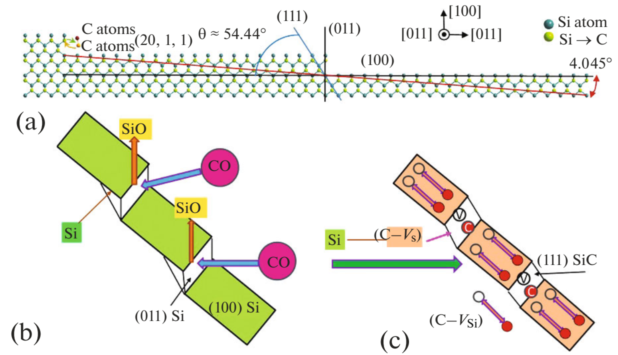

Fig. 9. Schematic representation of the mechanism of successive stages of the occurrence of reaction (1) on the vicinal Si(100) surface covered with (011) steps: (a) the vicinal Si(100) surface deviated by 4° in the [011] direction with (011) steps toward the $(11\bar{1})$ plane; (b) the initial Si(100) surface covered with (011) steps; and (c) the intermediate state formed during the transformation of the intermediate state into the SiC(111) plane, which lies at an angle of θ = 54°44′ to the (100) face.

pyramids). Note that the symmetry of these prisms is characteristic of both cubic and hexagonal symmetry crystals; that is, the symmetry is not degenerate. This means that both cubic and hexagonal symmetry crystals can grow on these surfaces. The result will depend only on thermodynamic conditions, i.e., on the temperature and densities of the falling streams of components from which the layer grows, rather than on the orientation of the substrate, which is extremely significant. If the hexagonal modification is stable under the given conditions, then the hexagonal modification will grow; if the cubic structure is stable, then the cubic modification will grow. This finding opens up completely new prospects for growing hexagonal semipolar crystals.

In addition, the authors of [41] discovered a fundamentally new mechanism of the occurrence of atomic substitution on *n*- and *p*-type conductivity vicinal Si faces deviated from the singular (100) face. The following was found: (i) an ordered SiC phase with the surface morphology in the form of facets (flakes) consisting of layers of both cubic and hexagonal phases is formed during SiC synthesis on the *p*-type conductivity vicinal Si surface deviated from the singular (100) face by an angle of ≥4°, and (ii) only an ordered cubic 3C-SiC phase is formed during SiC synthesis on the *n*-type conductivity vicinal Si surface deviated from the singular (100) face by an angle of ≥4°. This difference is attributed to the different mechanisms and rates of formation of dilatation dipoles and carbon–vacancy structures on the (100) face in Si doped with donor and acceptor impurities [41].

10. DRIFT MECHANISM OF EPITAXY OF SiC FILMS DURING THEIR GROWTH BY THE COORDINATED ATOMIC SUBSTITUTION METHOD ON A CRYSTALLINE Si SUBSTRATE: DIFFUSION MECHANISMS OF CO AND SiO MOLECULES IN Si

A new film growth mechanism via a topochemical reaction of the transformation of Si into SiC under the action of CO was theoretically proposed and experimentally confirmed in [50]. The main idea presented in [50] is as follows. The drift of CO molecules in a chemical reaction with Si initially occurs via the channels of the Si crystal saturated with dilatation dipoles C+V_{Si} and then via the SiC channels owing to the difference in the CO pressure outside and inside the crystal. In terms of this model, film growth is terminated when the SiO reaction product "clogs" the crystal channels and thereby decreases their hydraulic diameter. This is the fundamental difference between this model and the diffusion model, according to which the increase in the film thickness continues infinitely as $\sqrt{t}$. In the cited study, experiments on measuring the dependence of the maximum film thickness on Si(111) and Si(100) on pressure have been first conducted; it

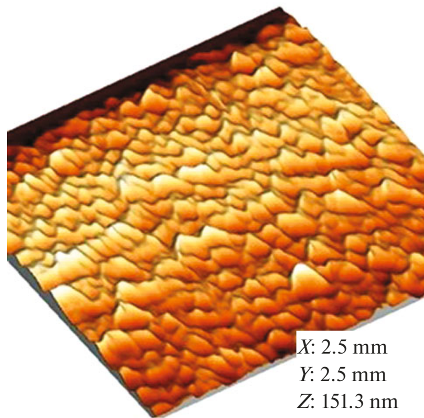

Fig. 10. Atomic force microscopy image of a SiC layer covered with (111) facets grown on the vicinal Si(100) surface deviated from the ⟨100⟩ direction by 4° toward *p*-type conductivity ⟨011⟩.

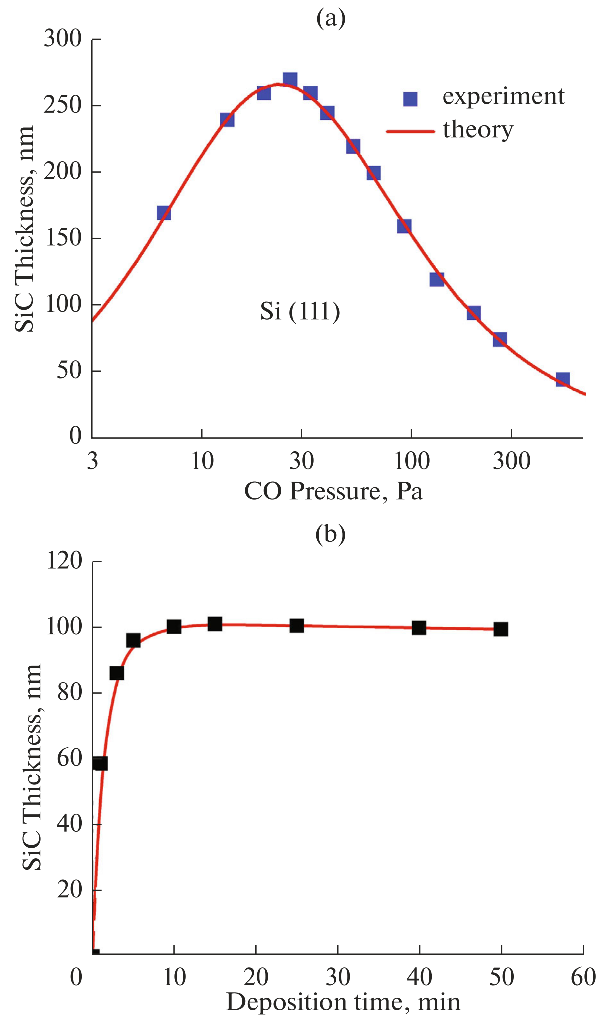

Fig. 11. Dependences of the final thickness of a SiC film on Si(111) on (a) the CO pressure (squares) and (b) growth time (squares). The solid lines stand for theoretical dependences calculated by formulas (12) and (11).

has been shown that there exists a pressure corresponding to the maximum film thickness. With a further increase in pressure, the film thickness decreases, whereas an opposite picture should be observed in the case of common diffusion growth, because the diffusion becomes even more enhanced. A general formula to describe the dependence of the thickness of a SiC film formed during topochemical growth has been derived in [50]. At a small time t, this dependence is a purely diffusion dependence:

$$L(t) = \sqrt{Dt}, \tag{10}$$

and at a large time, it has the form

$$L(t) = L_m\left[1 - \exp\left(-\frac{Dt}{2L_m^2}\right)\right], \tag{11}$$

$$L_m(P_{CO}) = L_*\frac{4P_{CO}/p_*}{\left[1 + (P_{CO}/p_*)^n\right]^2}, \tag{12}$$

where p_* and L_* are parameters with dimensions of pressure and length, respectively; n is the inverse polytropic exponent, $n = \frac{C - C_V}{C - C_p} = \frac{C - 2.5R}{C - 3.5R}$; $p_* = \left(\frac{p_0}{V\alpha}\right)^{\frac{1}{n}}$; $L_* = \frac{\pi(d_0/2)^2 p_*}{8\eta j_e}$; j_e is the volumetric equilibrium flow rate of the CO gas per unit area of the channel; and d is the hydraulic diameter of the channel. Figures 11a and 11b show dependences of the thickness of a SiC layer growing on the Si(111) face on the CO pressure and time, respectively. Similar curves for SiC growth on the Si(100) face can be found in [50]. It is evident from these data that, starting from a certain CO pressure, the increase in the layer thickness slows down, unlike the thickness of the layer growing owing to diffusion. Over time (at a fixed pressure), the increase in the layer thickness also ceases. Upon achieving a certain thickness, the layer does not grow any longer [50, 51].

The study of the diffusion of CO and SiO gases, which was begun in [50], was continued in [52, 53], where, using the methods of quantum chemistry, it was shown that vacancies V_{Si} and V_C and play a key role in the kinetics of reaction (1). The transport of the CO reagent gas to the reaction zone and the SiO gas—reaction product—from the reaction zone occurs only in the ⟨110⟩ direction and the equivalent directions, i.e., in the direction of the SiC channels. The migration of CO and SiO molecules is equivalent to the migration of the O atom and vacancies V_{Si} and V_C, because the migration of Si and C atoms is not man-

datory, since the O atom readily forms a chemical bond with any atom of the SiC crystal. The energy barrier to vacancy migration is more than 2 times lower than the barrier to atomic migration; in an ideal crystal, it is 3.6 eV for V_{Si} and 3.9 eV for V_C. Therefore, at low temperatures, the synthesis of SiC is limited to the migration of V_C. In a 3C-SiC crystal containing twin boundaries, the migration barriers can be lower by 10–20%. Starting from a temperature of 1100–1200°C, a significant portion of silicon vacancies will transit to carbon vacancies plus immobile carbon structures (activation energy for this process is 3.1 eV). Therefore, they can limit the SiC synthesis because of the lack of silicon vacancies. In this case, SiC synthesized by the coordinated atomic substitution method will contain both carbon clusters and traces of microexplosions caused by the accumulation of a large amount of SiO inside the SiC layer.

The diffusion and evolution of a porous layer were also studied in [54], where the time evolution of the average thickness of a porous layer in the case of exposure of the sample to a CO atmosphere was experimentally and theoretically studied and it was shown that, at the initial stages, the thickness is proportional to the cubic root of time. A model to describe the formation of a porous layer both at the initial stages, when the layer is represented by isolated pores, and at later stages, when the pores grow together and move inward as a single planar front, was proposed. It was theoretically shown that, in the latter case, the thickness of the porous layer is proportional to the square root of time.

11. THE POLYTYPISM OF SiC

According to all the above-cited studies, in particular, those that use the powerful apparatus of quantum chemistry [4], the main polytype formed during coordinated atomic substitution is the 3C-SiC cubic polytype. Figure 12 shows a typical—characteristic of most of the samples—XRD pattern recorded for a 3C-SiC sample grown on Si(111). The XRD pattern exhibits peaks attributed only to the (111) direction, which corresponds to pure epitaxy. This is quite obvious in terms of physics, because cubic silicon can undergo a coordinated transition only in a cubic SiC polytype. However, this does not mean that other SiC polytypes cannot be formed at certain time stages of the transformation of Si into SiC and on Si faces with an orientation different from (111). During a topochemical transformation, the 4H-SiC and 6H-SiC polytypes [4, 8, 10, 21, 26, 35, 44] and even the fairly rare 2H-SC and 8H-SiC polytypes can be formed (see Fig. 1 in [55]). Using a VUV-WASE ultraviolet ellipsometer (J.A. Woollam) equipped with a rotating analyzer in a range of 1.3–9.3 eV, the polytype composition of SiC films grown on Si by the coordinated atomic substitution method at T =

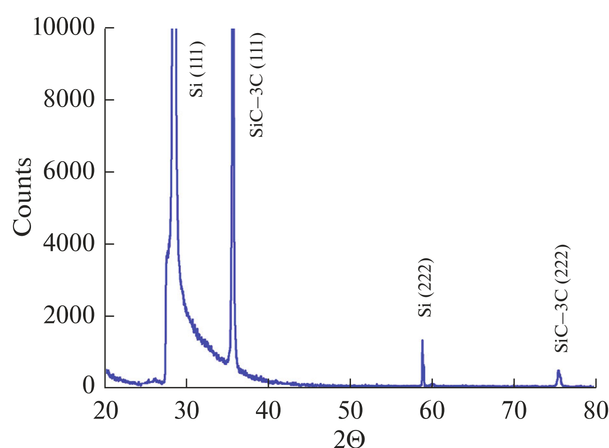

Fig. 12. X-ray diffraction pattern recorded for a 3C-SiC(111) sample grown on Si(111), which is typical of most of the samples.

1250°C, $p = 2$ Torr, and a growth time of 15 min was determined in [44]. It was shown that, under these conditions, the 3C cubic polytype is mostly formed on Si(111), the 4H hexagonal polytype with a small admixture of 3C is mostly formed on Si(110), and a mixture of the 3C, 6H, and 4H polytypes is formed on Si(100). On the basis of group-theoretical analysis, the formation of a new, previously unknown, trigonal (rhombohedral) SiC phase during the transformation of Si into SiC was theoretically predicted in [56]; this phase was experimentally detected in [57]. It was found that, if the synthesis time of SiC films does not exceed 5 min, then the Raman spectra exhibit, in addition to lines of 3C-SiC, a line at 258 cm^{-1}, which corresponds to the new intermediate rhombohedral SiC phase. The Raman spectra of the samples synthesized for more than 5 min did not exhibit this line.

12. THE ELASTIC PROPERTIES OF SiC FILMS SYNTHESIZED ON Si SUBSTRATES BY THE COORDINATED ATOMIC SUBSTITUTION METHOD

The elastic mechanical characteristics of nanoscale SiC/Si films were studied in [58, 59]. It was found that the upper thin SiC layers with a thickness of about 17 nm have a microhardness of 43 GPa, which is approximately 30% higher than the microhardness of bulk silicon carbide. Further, at a depth of 20–40 nm, the hardness abruptly decreases to a value equal to the microhardness of pure silicon. Young's modulus of the SiC film determined in [59] was 328 GPa, which is only slightly lower than Young's modulus of the C face of a bulk 4H-SiC crystal, which is 400 GPa [60].

13. ANOMALIES OF THE OPTICAL AND MAGNETIC PROPERTIES OF SiC FILMS GROWN ON Si BY THE COORDINATED ATOMIC SUBSTITUTION METHOD

13.1. Anomalies of Optical Properties

As noted above (Section 10), the main feature of SiC grown on Si by the coordinated atomic substitution method is the presence of carbon–vacancy structures in it, which are largely associated with the contraction or "collapse" of the material. However, it was found that the collapse leads not only to the formation of an ensemble of point defects. Upon the separation of Si from the silicon matrix, the silicon is subjected to an abnormally strong compression from the side of silicon carbide. The collapse corresponds to a phase transition from a metastable state with stretched bonds, in which four SiC cells coincide with four Si cells, to a stable SiC phase, in which five SiC cells coincide with four Si cells, and the degree of distortion of the Si–C bonds is significantly lower (about 0.2%). The pressure exerted by the stretched Si–C bonds on the nearest silicon layer can achieve 100 GPa. As a consequence of this contraction, every fifth chemical bond of SiC is fully consistent with every fourth bond of Si; the rest of the bonds undergo either rupture (leading to the formation of vacancies and pores) or compression. The latter apparently leads to a change in the structure of the surface zones of SiC adjacent to Si and the "metallization" or transformation of it into a "semimetal." In the case of doping of silicon carbide with boron atoms, the B atoms penetrate exactly into the voids of the carbon–vacancy structures (Fig. 4) and strongly change their properties. Figure 13 schematically shows the collapse of one layer with the initial lattice into the SiC lattice and a model of a carbon–vacancy dipole formed in SiC. Ellipsometic studies of SiC/Si samples grown on the (111), (110), and (100) faces of Si using a VUV-WASE ultraviolet ellipsometer (J.A. Woollam) equipped with a rotating analyzer in a range of 0.5–9.3 eV revealed the following. At the 3C-SiC(111)/Si(111) interface, an interface layer with completely new optical and electrical properties is formed. In principle, the optical properties of this interface cannot be described in terms of the Effective Media Approximation (EMA) [61, 62]. To describe these properties theoretically, it is necessary to use a model with oscillators that are in no way related to either SiC or Si. The best agreement with experiment was shown by the Tauc–Lorentz model, according to which the SiC/Si interface is a material with a zero band gap [61, 62]. Thus, it was found [61, 62] that a thin layer exhibiting semimetal properties that fundamentally differ from the properties of both SiC and Si is formed at the interface between 3C-SiC(111) and Si(111), and these properties cannot be described in terms of the EMA. This fact is attributed to the complex pattern of interaction of the two surfaces, where the SiC layer attracts individual Si atoms from the substrate, and the absence of misfit dislocations. As a consequence, an interface structure is formed (Fig. 13), where 88% of Si atoms at the interface form a chemical bond with atoms of the substrate, and 12% of Si atoms at the SiC(111) boundary do not form bonds, because they are too far from the Si atoms of the substrate. Using the methods of quantum chemistry, this structure was described in detail in terms of the density functional theory [61, 62] (Fig. 13). It was shown that *p* electrons of 12% of the Si atoms at the SiC(111) boundary with broken bonds provide a sharp peak in the density of electronic states exactly in the Fermi energy region (Fig. 14). In this case, the conduction band either touches the valence band or even penetrates into it as deep as about a few hundredths of an electron-volt, which approximately corresponds to the calculation error or is less than the error. It was shown that this theoretical representation is fully consistent with the experimental results on ellipsometry, according to which the optical properties of the layer at the 3C-SiC(111)/Si(111) interface correspond to the Tauc–Lorentz parameterization with a nearly zero band gap. The measured ellipsometric spectra show that the conductivity of the interface approximately corresponds to such metal as lead at electric field frequencies above 700 THz. At lower frequencies, the conductivity deteriorates.

The experiment showed that, in the samples of SiC films grown on the Si(100) surface, the formation of a layer exhibiting the properties of a semimetal is not observed, and the optical properties are described in terms of the simplest ellipsometric EMA model with high accuracy.

The samples of SiC films grown on the Si(110) surface had intermediate properties compared with the properties at the (111)–(110) interface. In this case, the formation of an interface with an extremely small (<0.5 eV)—yet in no way zero—band gap was observed on this surface.

All SiC samples grown on Si by the standard chemical vapor deposition method (samples from Anvil (United Kingdom) were studied), regardless of the substrate orientation, (111), (110), and (100), are described by the simplest ellipsometric EMA model with high accuracy. Even a trace of the presence of a "semimetal" was not detected in the samples.

13.2. Anomalies of Magnetic Properties

A set of experimental studies of magnetic properties, namely, the field and temperature dependences of the static magnetic susceptibility, for samples of single-crystal SiC thin films with a thickness of about of 80–100 nm that were grown on the (100), (110), and (111) surfaces of single-crystal Si by the coordinated atomic substitution method via a chemical reaction of silicon with carbon monoxide CO gas was conducted

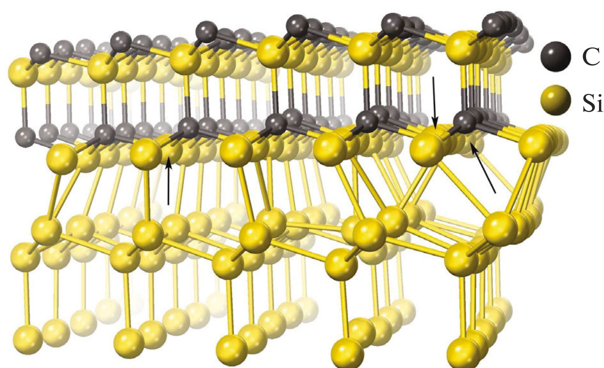

Fig. 13. Configuration of atoms at the dislocation-free 3C-SiC(111)/Si(111) interface corresponding to the minimum energy. The arrows indicate 3 out of 25 Si atoms that do not form bonds with atoms of the substrate. It is their *p* electrons that make the decisive contribution to the narrow peak of the density of electronic states in the vicinity of the Fermi energy (Fig. 14).

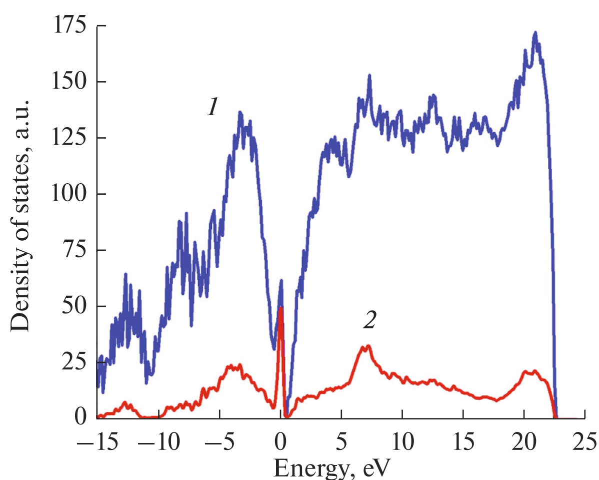

Fig. 14. Dependence of the density of electronic states of the studied system on energy (curve *1*). The Fermi energy corresponds to 0. Curve *2* is the contribution of the *p* electrons of the Si atoms at the SiC boundary that do not form bonds with the Si atoms of the substrate.

in [63]. The studies revealed the occurrence of two quantum effects in weak magnetic fields at room temperature in SiC structures grown on Si(110) and Si(111). These effects are (i) the formation of a hysteresis of the static magnetic susceptibility (Fig. 15a) and (ii) the occurrence of Aharonov–Bohm oscillations in the field dependences of the static magnetic susceptibility (Fig. 15b). The occurrence of the first of the effects is associated with the Meissner–Ochsenfeld effect; the second is associated with the presence of microdefects in the form of nanotubes and micropores in these structures under the SiC layer; the microdefects are formed during the synthesis of these structures and silicon in the above-discussed state of a "semimetal." In the SiC structures grown on Si(100), these effects were not detected; this fact is attributed to a different mechanism of SiC formation on the Si(100) surface, which was discussed above. Thus, the experimental studies have revealed for the first time the following nontrivial quantum effects at room temperature: the occurrence of the effect of quantization of the magnetic moment in SiC structures grown on Si(110) and Si(111) by the coordinated atomic substitution method and the formation of a hysteresis of the static magnetic susceptibility at room temperature in weak magnetic fields, which was interpreted by us as a manifestation of the Meissner–Ochsenfeld effect [63]. According to our reckoning, the occurrence of both the first and second effects is associated with the suppression of the electron–electron interaction by electric fields arising from microdefects consisting of dipole centers with a negative correlation energy and dipole centers of the edge channels of the SiC(111)/Si(111) structures. The occurrence of these effects is attributed to carbon–vacancy structures and the formation of a "semimetal" at the SiC/Si interface. Apparently, the manifestation of these effects can

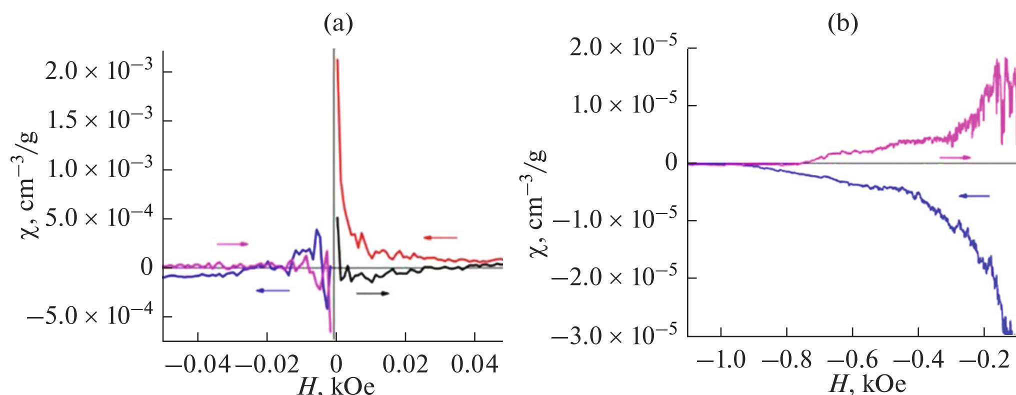

Fig. 15. Field dependences of static magnetic susceptibility exhibiting (a) a characteristic hysteresis in weak magnetic fields for the samples and (b) long-period Aharonov–Bohm oscillations in 3C-SiC(111)/Si(111) samples. The arrows indicate the scanning direction of the external magnetic field.

also be attributed to a special state of some of the Si atoms at the SiC(111)/Si(111) interface. In SiC structures grown on Si(100), where carbon–vacancy structures are hardly present at all and the interface is completely different, the above effects were not detected.

14. CONCLUSIONS

In this review, the main results concerning the technology and theory of SiC growth on Si by the coordinated atomic substitution method obtained by us after 2014 have been described. The physicochemical properties of SiC/Si structures have been described in detail. Unfortunately, owing to lack of space, our studies on the practical application of SiC/Si and the growth of a whole class of semiconductor compounds on SiC/Si substrates have not been touched upon at all. To date, epitaxial layers of AlN, GaN, AlGaN, ZnO, and ZnS wide-gap semiconductors have been grown on SiC/Si substrates. Epitaxial films of compounds of the entire series of A^2B^6 semiconductors have been grown. It has been experimentally shown that a SiC/Si substrate is quite suitable for growing filamentary nanocrystals of compounds of the A^3B^5 group. The AlN/SiC/Si, GaN/AlN/SiC/Si, and AlGaN/SiC/Si heterostructures have been used to construct some device structures, namely, pyrosensors and piezoelectric transducers; works on designing high electron mobility transistors have begun. Finally and most crucially, a semi-industrial technology for designing chips for light-emitting diodes on silicon has been developed for the first time, and a working prototype of a white light-emitting diode on silicon has been constructed.

ACKNOWLEDGMENTS

The studies were conducted using the equipment of the unique research setup Physics, Chemistry, and Mechanics of Crystals and Thin Films of the Institute of Problems of Mechanical Engineering of the Russian Academy of Sciences (St. Petersburg).

FUNDING

This work was supported by the Russian Science Foundation (project no. 20-12-00193).

CONFLICT OF INTEREST

The authors declare that there is no conflict of interest regarding the publication of this manuscript.

REFERENCES

1. Kukushkin, S.A. and Osipov, A.V., New method for growing silicon carbide on silicon by solid-phase epitaxy: model and experiment, *Phys. Solid State*, 2008, vol. 50, no. 7, pp. 1238–1245. https://doi.org/10.1134/S1063783408070081
2. Kukushkin, S.A., Osipov, A.V., and Feoktistov, N.A., RF Patent 2363067, 2009.
3. Kukushkin, S.A. and Osipov, A.V., *Nano-SiC na Si—novyi material dlya mikro- i optoelektroniki* (Nano-SiC on Si is a New Material for Micro- and Optoelectronics), Moscow: Inst. Probl. Tochn. Mekh. Upr., Ross. Akad. Nauk, 2006.
4. Kukushkin, S.A. and Osipov, A.V., Quantum mechanical theory of epitaxial transformation of silicon to silicon carbide, *J. Phys. D: Appl. Phys.*, 2017, vol. 50, art. ID 464006. https://doi.org/10.1088/1361-6463/aa8f69
5. Kukushkin, S.A. and Osipov, A.V., Thin-film heteroepitaxy by the formation of the dilatation dipole ensemble, *Dokl. Phys.*, 2012, vol. 57, no. 5, pp. 217–220. https://doi.org/10.1134/S1028335812050072
6. Kukushkin, S.A. and Osipov, A.V., A new mechanism of elastic energy relaxation in heteroepitaxy of monocrystalline films: interaction of point defects and dilatation dipoles, *Mech. Solids*, 2013, vol. 48, no. 2, pp. 216–227. https://doi.org/10.3103/S0025654413020143
7. Kukushkin, S.A. and Osipov, A.V., A new method for the synthesis of epitaxial layers of silicon carbide on silicon owing to formation of dilatation dipoles, *J. Appl. Phys.*, 2013, vol. 113, no. 2, art. ID 024909. https://doi.org/10.1063/1.4773343
8. Kukushkin, S.A. and Osipov, A.V., Anisotropy of the solid-state epitaxy of silicon carbide in silicon, *Semiconductors*, 2013, vol. 47, no. 12, pp. 1551–1555. https://doi.org/10.1134/S1063782613120129
9. Kukushkin, S.A. and Osipov, A.V., First-order phase transition through an intermediate state, *Phys. Solid State*, 2014, vol. 56, no. 4, pp. 792–800. https://doi.org/10.1134/S1063783414040143
10. Kukushkin, S.A. and Osipov, A.V., Theory and practice of SiC growth on Si and its applications to wide-gap semiconductor films, *J. Phys. D: Appl. Phys.*, 2014, vol. 47, art. ID 313001. https://doi.org/10.1088/0022-3727/47/31/313001
11. Kukushkin, S.A., Osipov, A.V., and Feoktistov, N.A., Synthesis of epitaxial silicon carbide films through the substitution of atoms in the silicon crystal lattice: a review, *Phys. Solid State*, 2014, vol. 56, no. 8, pp. 1507–1535. https://doi.org/10.1134/S1063783414080137
12. Kukushkin, S.A., Osipov, A.V., and Feoktistov, N.A., Chemical self-assembly of a single-crystal SiC film on a silicon substrate: a new method of directed nucleation, *Russ. J. Gen. Chem.*, 2013, vol. 57, no. 6, pp. 36–47.
13. Gordeev, S.K., Korchagina, S.B., Kukushkin, S.A. and Osipov, A.V., RF Patent 2286616, 2006.
14. Gordeev, S.K., Korchagina, S.B., Kukushkin, S.A., and Osipov, A.V., RF Patent 2286617, 2005.
15. Kukushkin, S.A., Osipov, A.V., Gordeev, S.K., and Korchagina, S.B., Nonequilibrium heteroepitaxy of sil-

icon carbide on silicon, *Tech. Phys. Lett.*, 2005, vol. 31, no. 10, pp. 859–861.
https://doi.org/10.1134/1.2121839

16. Zukov, S.G., Lukyanov, A.V., Kukushkin, S.A., Osipov, A.V., and Feoktistov, N.A., RF Patent 130996, 2013.
17. Kukushkin, S.A., Osipov, A.V., Rozhavskaya, M.M., Myasoedov, A.V., Troshkov, S.I., Lundin, V.V., Sorokin, L.M., and Tsatsul'nikov, A.F., Growth and structure of GaN layers on silicon carbide synthesized on a Si substrate by the substitution of atoms: a model of the formation of *V*-defects during the growth of GaN, *Phys. Solid State*, 2015, vol. 57, no. 9, pp. 1899–1907.
https://doi.org/10.1134/S1063783415090218
18. Kalinkin, I.P., Kukushkin, S.A., and Osipov, A.V., Effect of chemical treatment of a silicon surface on the quality and structure of silicon-carbide epitaxial films synthesized by atom substitution, *Semiconductors*, 2018, vol. 52, no. 6, pp. 802–808.
https://doi.org/10.1134/S1063782618060118
19. Kalinkin, I.P., Kukushkin, S.A., and Osipov, A.V., RF Patent 2323503, 2008.
20. *Handbook of Semiconductor Wafer Cleaning Technology: Science, Technology, and Applications*, Kern, W., Ed., Park Ridge, NJ: Noyes, 1993.
21. Kukushkin, S.A. and Osipov, A.V., Mechanism of formation of carbon–vacancy structures in silicon carbide during its growth by atomic substitution, *Phys. Solid State*, 2018, vol. 60, no. 9, pp. 1891–1896.
https://doi.org/10.1134/S1063783418090184
22. Kukushkin, S.A., Osipov, A.V., and Telyatnik, R.S., Elastic interaction of point defects in cubic and hexagonal crystals, *Phys. Solid State*, 2016, vol. 58, no. 5, pp. 971–980.
https://doi.org/10.1134/S1063783416050140
23. Eshelby J.D., Elastic inclusions and inhomogeneities, in *Progress in Solid Mechanics*, Sneddon, I.N. and Hill, R., Eds., Amsterdam: North-Holland, 1961, vol. 2, pp. 89–140.
24. Lifshits, I.M. and Rosentsveig, L.N., On construction of green's tensor for the basic equation of elasticity in the case of unbounded elastoanisotropic medium, *Zh. Vych. Matem. Fiz.*, 1947, vol. 17, no. 9, pp. 783–791.
25. Kuz'michev, S.V., Kukushkin, S.A., and Osipov, A.V., Elastic interaction of point defects in crystals with cubic symmetry, *Mech. Solids*, 2013, vol. 48, no. 4, pp. 431–438.
https://doi.org/10.3103/S0025654413040110
26. Egorov, V.K., Egorov, E.V., Kukushkin, S.A., and Osipov, A.V., Structural heteroepitaxy during topochemical transformation of silicon to silicon carbide, *Phys. Solid State*, 2017, vol. 59, no. 4, pp. 773–779.
https://doi.org/10.1134/S1063783417040072
27. Grudinkin, S.A., Kukushkin, S.A., Osipov, A.V., and Feoktistov, N.A., IR spectra of carbon-vacancy clusters in the topochemical transformation of silicon into silicon carbide, *Phys. Solid State*, 2017, vol. 59, no. 12, pp. 2430–2435.
https://doi.org/10.1134/S1063783417120186
28. Kukushkin, S.A., Nussupov, K.Kh., Osipov, A.V., Beisenkhanov, N.B., and Bakranova, D.I., X-ray reflectometry and simulation of the parameters of SiC epitaxial films on Si(111), grown by the atomic substitution method, *Phys. Solid State*, 2017, vol. 59, no. 5, pp. 1014–1026.
https://doi.org/10.1134/S1063783417050195
29. Kukushkin, S.A., Nussupov, K.Kh., Osipov, A.V., Beisenkhanov, N.B., and Bakranova, D.I., Structural properties and parameters of epitaxial silicon carbide films, grown by atomic substitution on the high-resistance (111) oriented silicon, *Superlattices Microstruct.*, 2017, vol. 111, pp. 899–911.
https://doi.org/10.1016/j.spmi.2017.07.050
30. Benemanskaya, G.V., Dementev, P.A., Kukushkin, S.A., Lapushkin, M.N., Osipov, A.V., Senkovskiy, B., and Timoshnev, S.N., Photoemission study of nano SiC epitaxial layers synthesized by a new method of the atom substitution in Si crystal lattice, *Mater. Phys. Mech.*, 2015, vol. 22, no. 2, pp. 183–190.
31. Kukushkin, S.A., Benemanskaya, G.V., Dementev, P.A., Senkovskiy, B., and Timoshnev, S.N., Synchrotron-radiation photoemission study of the ultrathin Ba/3C–SiC(111) interface, *J. Phys. Chem. Solids*, 2016, vol. 90, pp. 40–44.
https://doi.org/10.1016/j.jpcs.2015.10.018
32. Benemanskaya, G.V., Dementev, P.A., Kukushkin, S.A., Osipov, A.V., and Timoshnev, S.N., Carbon-based aromatic-like nanostructures on the vicinal SiC surfaces induced by Ba adsorption, *ECS J. Solid State Sci. Technol.*, 2019, vol. 8, no. 6, pp. M53–M59.
https://doi.org/10.1149/2.0031906jss
33. Davydov, S.Yu. and Lebedev, A.A., Vacancy kinetics in heteropolytype epitaxy of SiC, *Semiconductors*, 2007, vol. 41, no. 6, pp. 621–624.
https://doi.org/10.1134/S1063782607060012
34. Christian, J.W., *The Theory of Transformations in Metals and Alloys*, Oxford: Pergamon, 2002.
35. Sorokin, L.M., Veselov, N.V., Shcheglov, M.P., Kalmykov, A.E., Sitnikova, A.A., Feoktistov, N.A., Osipov, A.V., and Kukushkin, S.A., Electron-microscopic investigation of a SiC/Si(111) structure obtained by solid phase epitaxy, *Tech. Phys. Lett.*, 2008, vol. 34, no. 11, pp. 992–994.
https://doi.org/10.1134/S1063785008110278
36. Kukushkin, S.A. and Osipov, A.V., The Gorsky effect in the synthesis of silicon-carbide films from silicon by topochemical substitution of atoms, *Tech. Phys. Lett.*, 2017, vol. 43, no. 7, pp. 631–634.
https://doi.org/10.1134/S1063785017070094
37. Ratnikov, V.V., Kalmykov, A.E., Myasoedov, A.V., Kukushkin, S.A., Osipov, A.V., and Sorokin, L.M., Sequential structural characterization of layers in the GaN/AlN/SiC/Si(111) system by X-ray diffraction upon every growth stage, *Tech. Phys. Lett.*, 2013, vol. 39, no. 11, pp. 994–997.
https://doi.org/10.1134/S1063785013110230
38. Gorsky, W.S., Theorie des elastischen Nachwirkung in ungeordneten Mischkristallen (elastische Nachwirkung

zweiter Art), *Phys. Z. Sowjetunion*, 1935, vol. 8, pp. 457–471.

39. Kukushkin, S.A., Osipov, A.V., Bessolov, V.N., Medvedev, B.K., Nevolin, V.K., and Tcarik, K.A., Substrates for epitaxy of gallium nitride: new materials and techniques, *Rev. Adv. Mater. Sci.*, 2008, vol. 17, pp. 1–32.
40. Kukushkin, S.A. and Osipov, A.V., Phase equilibrium in the formation of silicon carbide by topochemical conversion of silicon, *Phys. Solid State*, 2016, vol. 58, no. 4, pp. 747–751.
https://doi.org/10.1134/S1063783416040120
41. Kukushkin, S.A., Osipov, A.V., and Soshnikov, I.P., Growth of epitaxial SiC layer on Si(100) surface of n- and p-type of conductivity by the atoms substitution method, *Rev. Adv. Mater. Sci.*, 2017, vol. 52, pp. 29–42.
http://www.ipme.ru/e-journals/RAMS/no_15217/05_15217_kukushkin.pdf
42. Grashchenko, A.S., Feoktistov, N.A., Osipov, A.V, Kalinina, E.V., and Kukushkin, S.A., Photoelectric characteristics of silicon carbide–silicon structures grown by the atomic substitution method in a silicon crystal lattice, *Semiconductors*, 2017, vol. 51, no. 5, pp. 621–627.
https://doi.org/10.1134/S1063782617050086
43. Kukushkin, S.A. and Osipov, A.V., Mechanism of formation of carbon–vacancy structures in silicon carbide during its growth by atomic substitution, *Phys. Solid State*, 2017, vol. 60, no. 9, pp. 1891–1896.
https://doi.org/10.1134/S1063783418090184
44. Kukushkin, S.A. and Osipov, A.V., Determining polytype composition of silicon carbide films by UV ellipsometry, *Tech. Phys. Lett.*, 2016, vol. 42, no. 2, pp. 175–178.
https://doi.org/10.1134/S1063785016020280
45. Grudinkin, S.A., Golubev, V.G., Osipov, A.V., Feoktistov, N.A., and Kukushkin, S.A., Infrared spectroscopy of silicon carbide layers synthesized by the substitution of atoms on the surface of single-crystal silicon, *Phys. Solid State*, 2015, vol. 57, no. 12, pp. 2543–2549.
https://doi.org/10.1134/S1063783415120136
46. Kukushkin, S.A., Nucleation of pores in brittle solids under load, *J. Appl. Phys.*, 2005, vol. 98, art. ID 033503.
https://doi.org/10.1063/1.1957131
47. Geguzin, Ya.E., *Diffuzionnaya zona* (Diffusion Zone), Moscow: Nauka, 1979.
48. Kukushkin, S.A. and Osipov, A.V., The equilibrium state in the Si-O-C ternary system during SiC growth by chemical substitution of atoms, *Tech. Phys. Lett.*, 2015, vol. 41, no. 3, pp. 259–262.
https://doi.org/10.1134/S1063785015030244
49. Kelly, A. and Groves, G.W., *Crystallography and Crystal Defects*, London: Longman, 1970.
50. Kukushkin, S.A. and Osipov, A.V., Drift mechanism of mass transfer on heterogeneous reaction in crystalline silicon substrate, *Phys. B* (Amsterdam), 2017, vol. 512, pp. 26–31
https://doi.org/10.1016/j.physb.2017.02.018
51. Kidalov, V.V., Kukushkin, S.A., and Osipov, A.V., Redkov, A.V., Grashchenko, A.S., Soshnikov, I.P., Boiko, M.E., Sharkov, M.D., and Dyadenchuk, A.F., Properties of SiC films obtained by the method of substitution of atoms on porous silicon, *ECS J. Solid State Sci. Technol.*, 2018, vol. 7, no. 4, pp. 158–160.
https://doi.org/10.1149/2.0061804jss
52. Kukushkin, S.A., Osipov, A.V., and Osipova, E.V., Mechanism of molecule migration of carbon and silicon monoxides in silicon carbide crystal, *Mater. Phys. Mech.*, 2019, vol. 42, pp. 178–182.
https://doi.org/10.18720/MPM.4222019_3
53. Kukushkin, S.A. and Osipov, A.V., Mechanism of diffusion of carbon and silicon monooxides in a cubic silicon carbide crystal, *Phys. Solid State*, 2019, vol. 61, no. 12, pp. 2338–2341.
https://doi.org/10.1134/S1063783419120242
54. Redkov, A.V., Grashchenko, A.S., Kukushkin, S.A., and Osipov, A.V., Kotlyard, K.P., Likhachevd, A.I., Nashchekind, A.V., and Soshnikov, I.P., Studying evolution of the ensemble of micropores in a SiC/Si structure during its growth by the method of atom substitution, *Phys. Solid State*, 2019, vol. 61, no. 3, pp. 299–306.
https://doi.org/10.1134/S1063783419030272
55. Kukushkin, S.A., Osipov, A.V., Romanychev, A.I., Kasatkin, I.A., and Loshachenko, A.S., Low-temperature growth of the CdS cubic phase by atomic-layer deposition on SiC/Si hybrid substrates, *Tech. Phys. Lett.*, 2020, vol. 46, no. 11, pp. 1049–1052.
https://doi.org/10.1134/S1063785020110085
56. Kitaev, Yu.E., Kukushkin, S.A., and Osipov, A.V., Evolution of the symmetry of intermediate phases and their phonon spectra during the topochemical conversion of silicon into silicon carbide, *Phys. Solid State*, 2017, vol. 59, no. 1, pp. 28-33.
https://doi.org/10.1134/S1063783417010164
57. Kitaev, Yu.E., Kukushkin, S.A., Osipov, A.V., and Redkov, A.V., A new trigonal (rhombohedral) SiC phase: ab initio calculations, a symmetry analysis and the Raman spectra, *Phys. Solid State*, 2018, vol. 60, no. 10, pp. 2066–2071.
https://doi.org/10.1134/S1063783418100116
58. Grashchenko, A.S., Kukushkin, S.A., and Osipov, A.V., Nanoindentation and deformation properties of nanoscale silicon carbide films on silicon substrate, *Tech. Phys. Lett.*, 2014, vol. 40, no. 12, pp. 1114–1116. https://doi.org/.10.1134/S1063785014120268
59. Grashchenko, A.S., Kukushkin, S.A., and Osipov, A.V., Study of elastic properties of SiC films synthesized on Si substrates by the method of atomic substitution, *Phys. Solid State*, 2019, vol. 61, no. 12, pp. 2310–2312.
https://doi.org/10.1134/S106378501412026859
https://doi.org/10.1134/S106378341912014X
60. Osipov, A.V., Grashchenko, A.S., Gorlyak, A.N., Lebedev, A.O., Luchinin, V.V., Markov, A.V., Panov, M.F., and Kukushkin, S.A., Investigation of the hardness and young's modulus in thin near-surface layers of silicon carbide from the Si- and C-faces by nanoindentation, *Tech. Phys. Lett.*, 2020, vol. 46, no. 8,

pp. 763–766.
https://doi.org/10.1134/S106378502008012X

61. Kukushkin, S.A. and Osipov, A.V., The optical properties, energy band structure, and interfacial conductance of a 3C-SiC(111)/Si(111) heterostructure grown by the method of atomic substitution, *Tech. Phys. Lett.*, 2020, vol. 46, no. 11, pp. 1103–1106.
https://doi.org/10.1134/S1063785020110243

62. Kukushkin, S.A. and Osipov, A.V., Anomalous properties of the dislocation-free interface between Si(111) substrate and 3C-SiC(111) epitaxial layer, *Materials*, 2021, vol. 14, no. 78, pp. 1–12.
https://doi.org/10.3390/ma14010078

63. Bagraev, N.T., Kukushkin, S.A., Osipov, A.V., Romanov, V.V., Klyachkin, L.E., Malyarenko, A.M., and Khromov, V.S., Magnetic properties of thin epitaxial SiC layers grown by the atom-substitution method on single-crystal silicon surfaces, *Semiconductors*, 2021, vol. 55, no. 2, pp. 137–145.
https://doi.org/10.1134/S106378262102007X

Translated by M. Timoshinina